COMPUTER AIDED PARAMETER EXTRACTION OF MOSFETS

By

CAPT AKHILESH KUMAR DAS

DEPARTMENT OF ELECTRICAL ENGINEERING

INDIAN INSTITUTE OF TECHNOLOGY, KANPUR

MARCH, 1985

COMPUTER AIDED PARAMETER EXTRACTION OF MOSFETS

A Thesis Submitted
In Partial Fulfilment of the Requirements
for the Degree of
MASTER OF TECHNOLOGY

By
CAPT AKHILESH KUMAR DAS

to the

DEPARTMENT OF ELECTRICAL ENGINEERING
INDIAN INSTITUTE OF TECHNOLOGY, KANPUR
MARCH, 1985

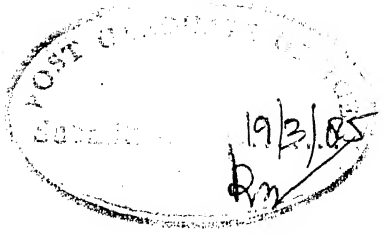

CERTIFICATE

This is to certify that this thesis entitled 'COMPUTER AIDED PARAMETER EXTRACTION OF MOSFETS' BY Capt. A.K. Das has been carried out under my supervision and has not been submitted elsewhere for a degree.

March 19 ,1985

(R. Sharan)
Professor
Department of Electrical Engineering
Indian Institute of Technology
Kanpur 208016, INDIA

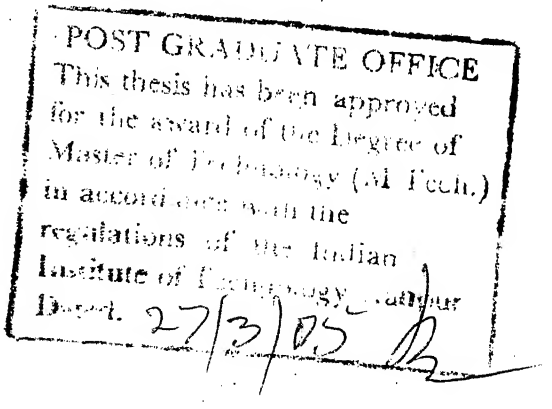

EE-1985-M-DAS-COM

ACKNOWLEDGEMENT

I wish to take this opportunity to express my deepest sense of gratitude to my supervisor Dr. R. Sharan who initiated me into this field. His sincere advice, keen interest and constructive criticism during the course of this work has been a perpetual source of encouragement.

I am also indebted to Mr. R.P. Gupta, and Mr. U. Mukhopadhyaya, my colleagues, for their invaluable time and support during the course of this work.

Thanks are also due to my wife who displayed a remarkable sense of resilence by keeping me away from the household chores, and my two children who showed a remarkable appetite for the manuscript copy of this work. May be they understood, what it was all about !

Finally, I deeply appreciate the excellent typing done by Mr. J.S. Rawat.

- Capt Akhilesh Kumar Das

LIST OF SYMBOLS

V_G = Gate potential

V_D = Drain potential

V_s = Source potential

V_b = Substrate potential

W = Channel width

L = Channel length

T_{ox} = Oxide thickness

Q_s = Total induced charge/unit area in the silicon substrate

Q_d = Fixed negative charge in the depletion layer due to ionised impurity atoms

V_{tx} = effective threshold voltage

Q_{ss} = equivalent insulator charge

Q_m = mobile negative charge

E_{ox} = Relative permitivity of the oxide material x E_o

E_{si} = Relative permitivity of silicon x E_o

E_o = Permitivity of free space

ϕ_{ms} = metal-semiconductor work function difference

ϕ_f = Fermi potential of the substrate

μ = mobility of carrier

q = electronic charge

V_{sat} = pinch off voltage

N_A = doping concentration of (p type substrate)N Chl MOSFET

N_D = doping concentration of (n type substrate)P Chl MOSFET

γ = imperical constant

V_{TO} = Threshold voltage

CGD = Gate-drain capacitance

CGS = Gate-source capacitance

ABSTRACT

In this thesis entitled 'COMPUTER AIDED PARAMETER EXTRACTION OF MOSFETS', the parameters characterising the electrical behaviour of N and P channel enhancement mode MOSFETS have been determined.

The device model chosen is the one developed by J.E. Meyer [1]. The model when extended to the device under study has three parameters and a single independent variable.

The data points were obtained from the experimentally observed I-V characteristics of the transistors.

The parameters were extracted using the Nonlinear least square curve fitting algorithm suggested by Levenberg Marquardt [2]. The program for the same was developed as a part of the project.

The parameters thus extracted were put to rigorous validity checks including checks with 1/f noise measurements to ascertain their physical consistency. The results justify the scheme adopted for study.

References

1. MOS MODELS and CIRCUIT SIMULATION - John E. Meyer RCA Review, vol. 32, Mar 1971.

2. COMPACT NUMERICAL METHODS FOR COMPUTERS - J.C. Nash; Adam Hilger Ltd., Bristol.

TABLE OF CONTENTS

CHAPTER 1

INTRODUCTION

The CMOS technology is here to stay, as it finds tremendous favour with the manufacturers of LSI and VLSI components. It is not surprising therefore that considerable work is being done in this field to study the device behaviour over a myriad set of operating ranges and variables. Many aspect of device behaviour continue to elude theoretical explanations. Various models of device have been suggested and will continue to be formulated to define the device behaviour as accurately as possible.

The behaviour of the device is determined by the external variables such as temperature, voltage, current, circuit configuration in which the device is used, type of load etc., as also by the physical parameters of the device, such as doping density, geometry of the device, type of semiconductors used etc. while the external variables are easily determined; it is the physical parameters of the device which are not so easily found. The manufacturers either by design or accident do not dwell on the physical parameters, that would help define the device behaviour in totality.

The converse is also true. If a device with a certain behaviour be required, it is absolutely essential to establish a cause-effect correlation during the manufacturing process . The 'cause' corresponding to the device parameters and 'effect' to the device behaviour.

Therefore schemes have to be developed by users and manufacturers of the device to extract the device parameters, and thus provide a bridge over a vital information gap.

Breadboarding used to be a common scheme for parameter extraction of discrete devices, since these entailed fewer variables, simpler models and usually operated in domains where theories are well established. However the advent of LSI and VLSI technology has as a matter of need ushered in a new era of computer aided simulation. The models required have to be very accurate, since a slight inaccuracy in a single stage of the chip, may have a drastic effect on the overall behaviour of the chip. The accuracy desired in parameter extraction for CAD application too,is of a high order.

The device chosen for the study in this project is CMOS inverter CD4007. It has three inverters of which one is internally connected and in the remaining two NMOS and PMOS pair are left without internal connection. Some data has also been taken on the high speed CMOS 74HC04.

The device model chosen in the case of CD4007 is the one developed by J.E. Meyer [1]. The model is discussed in Chapter 2. Some basic device physics concepts shaping the evolution of this model are described in Appendix A.

The I-V relationship as propounded by J.E. Meyer for N and P channel are nonlinear within the parameters. Hence the parameters extraction algorithm has to be a nonlinear one. The algorithm chosen for parameters extraction is the one suggested by Levenberg-Marquardt [2],[3]. The Levenberg-Marquardt algorithm is a combination of Gauss-Newton and steepest descent methods. This algorithm provides the best tradeoff between computation time and accuracy of initial guess to be provided to it as input. The optimisation scheme is discussed in Chapter 3. The algorithm for the program is listed at Appendix B.

The parameters thus extracted are discussed in Chapter 4. A comparative study of the expected values and obtained values are carried out. The consistency or lack of it for the obtained parameters, over a different set of data points are also described in this chapter. The validation and error analysis are also carried out in this chapter. The validation of the parameters have been carried out by

a) numerically generating the I-V characteristics of N channel and P channel, and ensuring point to point coincidence with experimental I-V characteristics

b) numerically generating the transfer characteristics of CMOS inverter comprising of the two transistors and comparing it with actual transfer characteristics.

Also the spectral power density for 1/f noise [4] of N channel Mosfet has been analysed. This analysis shows a fair agreement with established theories. In Chapter 5 the entire work has been summarised and suggestion for further work in this field have been incorporated.

CHAPTER 2

MODEL OF MOSFETS

For computer aided simulation one of the most important ingredients is the model of the device. While there are no dirth of models that have been suggested for MOSFETS, the choice of a particular model depends mainly on the 'aspects of study' of the device one is interested in, be it D.C., A.C. transient, noise behaviour or any other field. Some models may involve parameters that may cover the wide range of operation of the device, while others have been formulated with a certain bias to the field of study. Further one will do well, to chose those models which have a well established theory rather than a pure empirical model.

In this project the model chosen for parameter extraction, is the one developed by J.E. Meyer. In this chapter we will focus our attention to some of the salient features of this model. The basic device physics concepts contributing to the evolution of this model have been listed in Appendix A.

2.1 TRIODE REGION:

The structure of a typical N channel Mosfet has been illustrated in Fig. 1. Let the potentials at gate drain, source and substrate be V_g, V_d, V_s and V_b respectively. Further

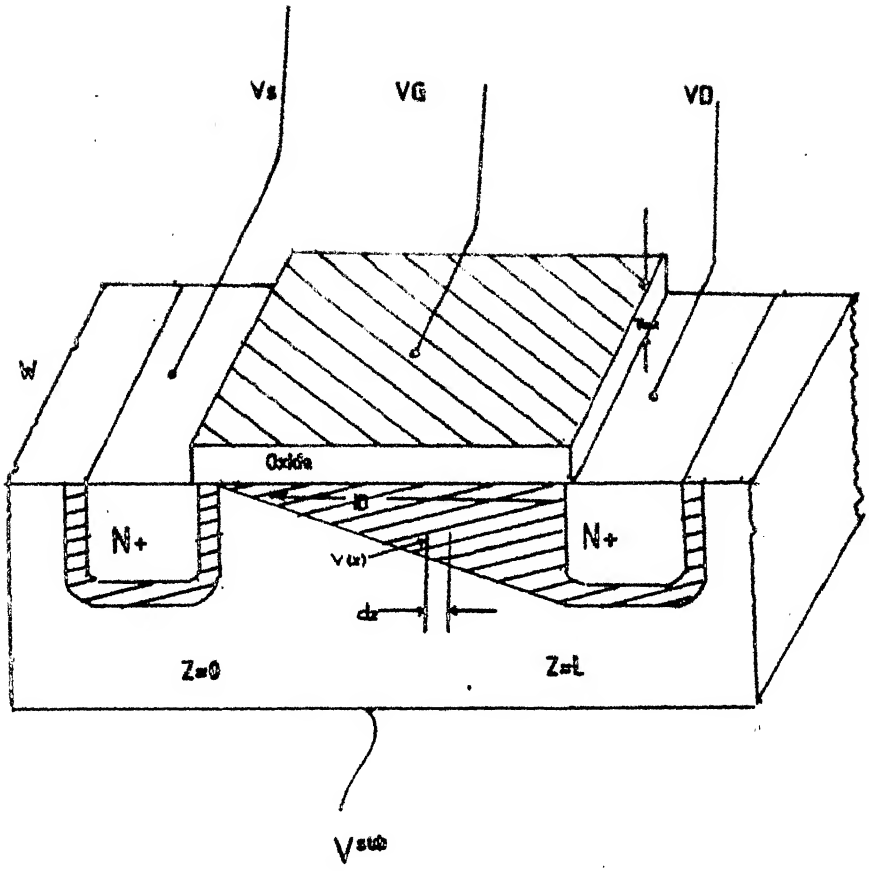

NMOS STRUCTURE

FIG-1

let V(z) be the potential at the surface of the channel and W, L, and T_{ox} be the channel width, source drain spacing, and oxide thickness respectively. At a distance 'Z' from the source the total charge per unit area Q_s, induced in the silicon substrate will consist of a mobile negative charge Q_m in the surface inversion layer and a fixed negative charge Q_d, in the underlying depletion region, due to ionised impurity atoms.

Thus

$$Q_m(z) = Q_s(z) - Q_d(z) \quad \ldots \quad (1)$$

By Gauss' Law

$$Q_s(z) = -\frac{E_{ox}}{T_{ox}} (V_g - Vtx - V(z)) \quad (2)$$

and

$$Q_d(z) = -\sqrt{2\, E Si q N (V(z) - V_b + 2\phi F)} \quad (3)$$

Equation (2) relates the total charge in the silicon to the impressed field $V_g - V(z)$ and an effective threshold voltage V_{tx}. This effective threshold voltage includes the contribution of metal-semiconductor work-function difference ϕ_{ms}, the Fermi potential of the substrate ØF and the equivalent insulater charge Q_{ss}. Thus,

$$V_{tx} = 2\,\phi f - \phi_{ms} - \frac{Q_{ss}}{C_{ox}} \quad (4)$$

Eqn. (3) relates the charge of ionised impurity to the channel-substrate potential. The voltage drop across an elemental section of the channel is given by

$$dv = IdR = \frac{-Id\ dz}{W\mu Q_m(z)} \qquad (5)$$

substituting equations (1),(2),(3) and (4) in equation (5) and integrating

$$-\int_0^L Id\ dz = \int_{V_s}^{V_d} \frac{W\mu E_{ox}}{T_{ox}} [-(V_g-V_{tx}-V(z)))$$

$$+ \frac{T_{ox}}{\varepsilon_{ox}} \sqrt{2\varepsilon_{Si} qN(V(z)-V_b+2\phi f}]dV \qquad (6)$$

$$Id = K[-(V_g-V_{tx}-V(z))^2 - \frac{4}{3}R(V(z)-V_b+2\phi f)^{3/2}]_{V_s}^{V_d} \qquad (7)$$

where

$$K = \frac{\mu E_{ox}}{2LT_{ox}} \qquad (8)$$

$$R = \frac{T_{ox}}{E_{ox}} \sqrt{2 E_{Si} qN} \qquad (9)$$

2.2 SATURATION REGION:

Eqn. (7) establishes relationship of drain current with V_g, V_b, V_s and V_d in triode region of operation. The

saturation region behaviour demands that the entire channel be inverted. This implies that the entire term in square bracket in eqn. (6) (the mobile channel charge) must be negative for all z, thus giving the following relationship

$$(V_g - V) \leq V_{tx} + R\sqrt{V - V_b + 2\phi f} \qquad (10)$$

The saturation voltage V_{sat} can be determined by solving the above equation by substituting V_{sat} for V and applying equality.

V_{sat} thus determined, defines the drain voltage V_d at which $Q_m(z)$ at the drain becomes zero. Since in practice $Q_m(z)$ cannot become zero, implying zero drain current, so an approximation has been made. This approximation indicates that beyond pinchoff, the drain conductance becomes zero while the drain current remains constant at a value equal to that achieved at pinch off. However as will be noted from typical device characteristics, the drain conductance is by no means zero in the saturation region. This conductance is generally attributed to two feedback mechanisms by which a change in drain voltage can effect the drain current.

The first mechanism is due to a spreading of depletion region near drain, which results in a reduction

of active channel length. The second mechanism by which a change in drain voltage can effect the drain current is by electrostatic coupling of the drain contact region to channel. For the purpose of computer aided analysis it is usually sufficient to define the drain current empirically.

$$Ids = Id_{sat} (1 + \gamma \cdot V_{DS}) \qquad (11)$$

when $I_{D\ sat}$ is drain current at $V_D = V_{sat}$.

2.3 MOBILITY REDUCTION:

With the increase in gate source bias, or drain source supply there is a decrease in inversion layer mobility due to diffuse surface scattering. This reduction in mobility can be accounted for in an empirical fashion.

$$\mu_{eff} = \mu_{eff}(o) \left(\frac{E_{so}}{E_s}\right)^q \qquad (12)$$

when $E_{so} = 6 \times 10^4$ V/cm

$\mu_{eff}(o)$ = Constant (low field) mobility for $E_s < E_{so}$

q = an empirical constant (usually between .08- .25)

$$E_s = -(V_{gs} - V_{tx} - \frac{V_{DS}}{2})/T_{ox} \qquad (13)$$

2.4 CURRENT AND VOLTAGE RELATIONSHIP OF MEYER'S MODEL WHEN EXTENDED TO DEVICE UNDER STUDY:

The J.E. Meyer's model also account for voltage dependent capacitances. Since these are not pertinent to the

extraction of parameters determining the d.c. behaviour of the device, no attempt is made here to dwell on these.

The device used for study is CD-4007. On this I.C. all substrates and source for both N and P channel are internally connected. To determine the I-V characteristics of the device these in turn have been grounded. Thus we have

$$V_s = V_b = 0 \tag{14}$$

Solving eqn. (7) we have for the N channel

$$I_{ds} = K \left[\frac{4}{3}R(2\phi f)^{3/2} - V_{DS}^2 + 2(V_{GS}-V_{tx})V_{DS} \right.$$

$$\left. - \frac{4}{3} R(V_{DS}+2\phi f)^{3/2} \right] \tag{15a}$$

The drain current for the P channel

$$I_{SD} = K \left[\frac{4}{3} R(2\phi f)^{3/2} - V_{SD}^2 + 2(V_{SG}-V_{tx})V_{SD} \right.$$

$$\left. - \frac{4}{3} (V_{SD}+2\phi f)^{3/2} \right] \tag{15b}$$

The saturation voltage for the two N and P channel transistors are obtained by solving eqn. (10).

$$V_{DSAT}(N_{chl}) = (V_g-V_{tx}) + \frac{R^2}{2} - \frac{R}{2}\sqrt{(R^2-4V_{tx}+4V_{GS}+8\phi f)} \tag{16a}$$

$$V_{DSAT}(P_{chl}) = (V_{SG}-V_{tx}) + \frac{R^2}{2} - \frac{R}{2}\sqrt{R^2-4V_{tx}+4V_{SG}+8\phi f)} \quad (16b)$$

The saturation current for the two are exactly as indicated in eqn. (11) i.e.

$$I_{DS}(N_{chl}) = I_{d\ sat}(1+\gamma.V_{DS}) \quad (17a)$$

$$I_{SD}(P_{chl}) = I_{dsat}\ (1+\gamma.V_{SD}) \quad (17b)$$

The mobility degration for both the transistors are accounted for by eqn. (12), which is reproduced below.

$$\mu_{eff} = \mu_{eff}(o)\ (\frac{E_{so}}{E_s})^q \quad (18)$$

Thus eqns. (15), (16), (17) and (18) define the d.c. behaviour of the two N and P MOSFETS.

Examining the above equations, we have the following parameters, which when determined, can be used to simulate the device behaviour.

$$K = \frac{\mu E_{ox} W}{2LT_{ox}} \quad (19)$$

$$R = \frac{T_{ox}}{E_{ox}}\sqrt{2qE_{Si}N} \quad (20)$$

$$2\phi f = \frac{KT}{q}\ \ln\frac{N_a}{n_i} \quad (21)$$

γ = conductance parameter in saturation

q = mobility degradation factor

V_{TO} = Threshold voltage = $R\sqrt{2\phi f} + 2\phi f$ (22)

2.5 EXTENSION OF EXTRACTED PARAMETERS TO SPICE:

In the simulation program SPICE, the MOSFET model is derived from the FROHMAN-GROVE model. The d.c. characteristics of the MOSFET are defined by the parameters, VTO, BETA, LAMBDA, PHI and GAMMA, where

GAMMA = Bulk threshold parameter

VTO = Zero bias threshold voltage

BETA = Intrinsic transconductance parameters

PHI = Surface potential at strong inversion

LAMBDA = Channel length modulation parameter.

Interestingly J.E.Meyer's model is used in SPICE to determine the voltage dependent capacitance.

If we examine the inputs to SPICE we find that these are either exactly identical or at best have a minor variation to the parameters being highlighted in Meyer's model. (For the simulation of a device, the above mentioned parameters have to be provided to SPICE. This is not easy, and hence the SPICE assumes certain default values, which are bound to be in error with the actual device parameters and

the device simulation at best is approximate). A quick look at the table below establishes the correspondence between the SPICE model parameters for MOSFETS and the MOSFET parameters highlighted by Meyer's model.

SPICE PARAMETERS	RELATION WITH MEYER'S PARAMETERS
1) VTO = ZERO BIAS THRESHOLD VOLTAGE	$= R\sqrt{2\phi_f + 2\phi_f}$
2) BETA= INTRINSIC TRANS CONDUCTANCE PARAMETER	$= f(K)$ where $K = \frac{\mu E_{ox} W}{2LT_{ox}}$
3) PHI= SOURCE POTENTIAL AT STRONG INVERSION	$= \phi = (PHI)$
4. GAMA= BULK THRESHOLD PARAMETER	$= f(R)$ where $R = \frac{T_{ox}}{E_{ox}} \sqrt{2q E_{s_i} N}$
5) LAMBDA= CHANNEL LENGTH MODULATION	accounted for by mobility reduction expressions.

CHAPTER 3

NONLINEAR LEAST SQUARE METHOD

Having provided the model of the device and defined the parameters to be extracted, it is imperative to think of how to extract these parameters. While this problem can be attacked from many a direction, the best choice probably is to see the problem as one of 'curve fitting'. This class of problem offers a multiplicity of choice by way of standard algorithm, and a few library subroutines. Before one choses a particular algorithm the compatability of the model to the extraction algorithm has to be established.

If we examine equation(15a) of Chapter 2 we have

$$I_{ds} = K[4/3R(2\phi f)^{3/2}+2(V_{GS}-V_{tx})V_{DS}-V_{DS}^{2} - 4/3\ R(V_{DS}+2\phi f)^{3/2}] \qquad (1)$$

This equation is of a classic mathematical form.

$$Y = F(X_1,X_2\ldots X_K;\ A_1,A_2\ \ldots\ A_M) \qquad (2)$$

having K independent variable, and M parameters. A point of interest that is revealed by examining equation (1) is that the equation is nonlinear in parameters (also in independent

variables), and hence one will have to choose essentially a nonlinear method. The nonlinear methods are iterative in nature in which the starting values are picked up, upgraded by the algorithm untill a convergence criteria is satisfied. Some of the common nonlinear methods used are

1. Steepest Descent
2. Gauss-Newton algorithm
3. Levenberg-Marquandt's algorithm
4. Davidson Fletcher and Powell's algorithm and others.

Examining these algorithms it was realised that the Levenberg-Marquardt's algorithm offerred the best choice. The Levenberg-Marquardt algorithm is a combination of Gaus-Newton and Steepest descent, The Levenberg-Marquardt's algorithm aims to capitalise on the best features of these algorithm while rejecting their individual pit falls.

3.2 THE LEVENBERG-MARQUARDT'S ALGORITHM:

Regardless of whether the equation is linear or nonlinear in the parameters, usually the criteria for obtaining the best model parameters are commonly satisfied by the least squares objective function.

$$S = \sum_{i=1}^{N} (Y_i - Y_i^*)^2 \qquad (3)$$

when Y_i^* = predicted or calculated value of dependent variable for the ith observation

N = No. of data points

Y_i = Experimental value of the dependent variable for the ith observation.

The best model parameters are obtained when the objective function is minimised

$$\frac{d_\Sigma}{d_{AJ}} = 0, \quad J = 1,2,\ldots M \tag{4}$$

All algorithms aim to minimise the least square objective function and differ only in the route they follow to upgrade parameters from one iteration to another iteration.

Focussing attention to the problems in hand we have in essence a classical mathematical function.

$$Y = F(X_1, X_2 \ldots X_k, A_1, A_2 \ldots A_m) \tag{5}$$

$$Y = F(\bar{X}, \bar{A}) \tag{6}$$

where $\bar{X} = (X_1, X_2 \ldots X_k)$

$\bar{A} = (A_1, A_2 \ldots A_m)$.

Aim is to determine $\bar{A}$, that would provide the best fit to the experimental data. The Gauss Newton algorithm and the Steepest Descent algorithm differ in the rules for

upgrading the vector $\underline{A}$ from kth iteration to (k+1)th iteration. The incremental vector ΔA that updates the parameter values from one iteration to another is related as follows.

$$K\, B\, \Delta A = J^T(Y-Y^*) \qquad (5)$$

In case of steepest descent

B is an identity matrix

K is a step length.

This is obtained by assuming only the first order terms in the Taylor series expansion $Y = f(X,A)$ at some value of X and A and substituting the values in eqn. (4).

In case of Gauss Newton

$K = 1$

$B = J^T J$

This is obtained by selecting the first and second order terms of Taylor series expansion for $Y = f(\underline{X},\underline{A})$ where J = Jacobi matrix

$$J = \begin{matrix} \frac{\partial Y_1^*}{\partial A_1} & \frac{\partial Y_1^*}{\partial A_2} & \cdots & \frac{\partial Y_1^*}{\partial A_M} \\ \frac{\partial Y_2^*}{\partial A_1} & & & \\ \frac{\partial Y_N^*}{\partial A_1} & \cdots & \cdots & \frac{\partial Y_N^*}{\partial A_M} \end{matrix} \qquad (6)$$

J^T = Transpose of Jacobi

$$(Y-Y^*) = \begin{matrix} Y_1 - Y_1^* \\ Y_2 - Y_2^* \\ \vdots \\ Y_N - Y_N^* \end{matrix} \qquad (7)$$

$$\Delta A = \begin{matrix} A_1 - A_1^* \\ A_2 - A_2^* \\ \vdots \\ A_M - A_M^* \end{matrix} \qquad (8)$$

The Levenberg-Marquardt's algorithm combines the two algorithms to yield

$$(J^TJ + \lambda D^2) \quad A = J^T (\underline{Y - Y^*})$$

where λ = Marquardt's parameter

D^2 = scaling vector $(J^TJ)_{ii} + \phi$

ϕ = 1.0 is Nash parameter; introduced to circumvent failures when one of the diagonal elements of J^TJ is zero.

In general a steepest descent procedure is expected to converge for poor starting values, but requires lengthy

solution time, because of its tendency to criss-cross a valley on the function S, instead of following the floor of the valley to a minimum. The primary cause of this is, that the search directions generated are not linearly independent.

Gauss-Newton on the other hand will converge rapidly for good starting guesses. In the Levenberg-Marquardt's algorithm initial value of lambda (λ) are large and decrease towards zero as the optimum is approached. The rules for calculating have been heuristically determined. These are

a) λinitial = 001

b) If the objective function at the end of a given iteration; calculated with the upgraded value of parameters (S new) is greater than the objective function at the beginning of the in iteration (S old) then

λ new = λold * 10.0

This implies that the upgraded values of parameters at the end of a given iteration shows a negative trend to the one desired since the least square error is enhanced. By increasing lambda (λ) one is tending more towards steepest descent.

c) If the objective function at the end of the given iteration (S new) is less than S old then

$$\lambda_{new} = \lambda_{old} * 0.4$$

This decision reflects the fact that the upgraded parameters show a favourable trend towards convergence. By decreasing λ (lambda) one is tending more towards Gauss Newton.

3.2 SUITABILITY OF THE ALGORITHM:

In a typical extraction procedure, parameters are usually extracted sequentially, one at a time in small groups [5]. The value of each parameter is assumed fixed and accurate for use in extracting further parameters. A small portion of the model and data from a limited part of devices operating ranges are used in extracting each parameters, using the least square minimisation criteria.

Several difficulties may be encountered with this procedure. First the sequential approach to parameter extraction does not take into account the interaction of parameters. Also the parameters obtained from the limited range of the device may not correctly define the device behaviour in other range of operation. Another problem is that some parameters which have a large impact on the simulated characteristics, may be deeply imbedded in the model equations.

The result of these problems are that the model does not give the full accuracy of which it is capable of. A final difficulty is that the parameters extraction routines must be tailored to a specific device model which can produce a significant overhead in modifying or replacing a model.

The Levenberg-Marquardt algorithm is a multi-variable regression algorithm and is thus able to attack all the parameters simultaneously. The data points selected are for the entire triode region, and thus the usual problems found with other techniques are negotiated at the same time. The choice of Levenberg-Marquardt's algorithm is thus vindicated.

3.3 PROBLEMS PECULIAR TO MOSFET PARAMETER EXTRACTION:

Most models are based on physical theory but there are always some parameters which do not have physically well defined values, and others for which the physical values do not yield best fit to the device characteristics. Model parameters extraction using experimentally observed data points is the obvious solution to this problem.

In order to be useful on a routine basis any parameter extraction algorithm must produce parameters

reliably and accurately. Two potential sources of error in the optimisation technique described, are [5].

a) local minima

b) Redundancy/Insensitivity of parameters

The first can result in non-optimum parameter values, and the second can produce non-unique parameter values, but yet give an optimum fit to the data. The latter is essentially a feature of the model equation.

The accuracy in locating the minima is primarily determined by the convergence criteria. More strict the convergence tolerance, more accurate are the results, but this will need more computation time.

The redundancy problem can be tackled by good initial guesses for the parameters; coupled with constrained minimisation. Constrained minimisation implies that a bound has to be placed on upper and lower limits of the parameter values and also the sign of the values.

3.4 THE CONVERGENCE CRITERIA:

In the preceding paragraph we have asserted the importance of a judicious choice of convergence criteria. Some of the common convergence criteria that are usually chosen are:

a) The objective function value falls below a predetermined value.

b) The relative change in objective function value from one iteration to another, is less than same specified value.

c) The change in each parameters from one iteration to the next is within some specified value.

d) No adjustment of can be found that reduces the error.

The convergence criteria chosen in this case is a combination of criteria mentioned in subpara (a) and (c) above. i.e.

$$\frac{\Delta A}{A} < 1E\text{-}7$$

$$S < 1E\text{-}7$$

The above twin conditions have to be jointly satisfied for convergence to be achieved. The justification for the choice is listed below.

The scheme has been developed for extracting three parameters.

$$A(1) = K = \frac{\mu E_{ox} W}{2L T_{ox}}$$

$$A(2) = R = \frac{T_{ox}}{\varepsilon_{ox}} \sqrt{2q E s_i N}$$

$$A(3) = 2\phi f$$

The expected values of:

A(1) is in the neighbourhood of 1E-3

A(2) is in the neighbourhood of 1E0

A(3) is in the neighbourhood of 1E0

Therefore a change in these parameters by a quantity less than 1E-7 is indicative of the fact that the change is less than .001%, meaning thereby that further refinements, except for aesthetics have little influence on the parameters.

Further the number of data points chosen for extracting these parameters were taken to be ≤10. The value of dependent variable (I_{DS}/I_{SD}) showed a spread from (.1-10)E-3 amps. An objective function less than 1E-7 implies an error of less than .1 ma between the data points numerically generated and data points experimentally observed. This order of error can easily be accounted to the measurement technique used.

The two criteria put together are expected to give fairly consistent results over various sets of data points.

Also to check the otherwise divergent tendency of the program a constraint [6] was imposed on the sign of the parameters. All parameters values extracted were expected to be positive. Hence, during the course of a iteration

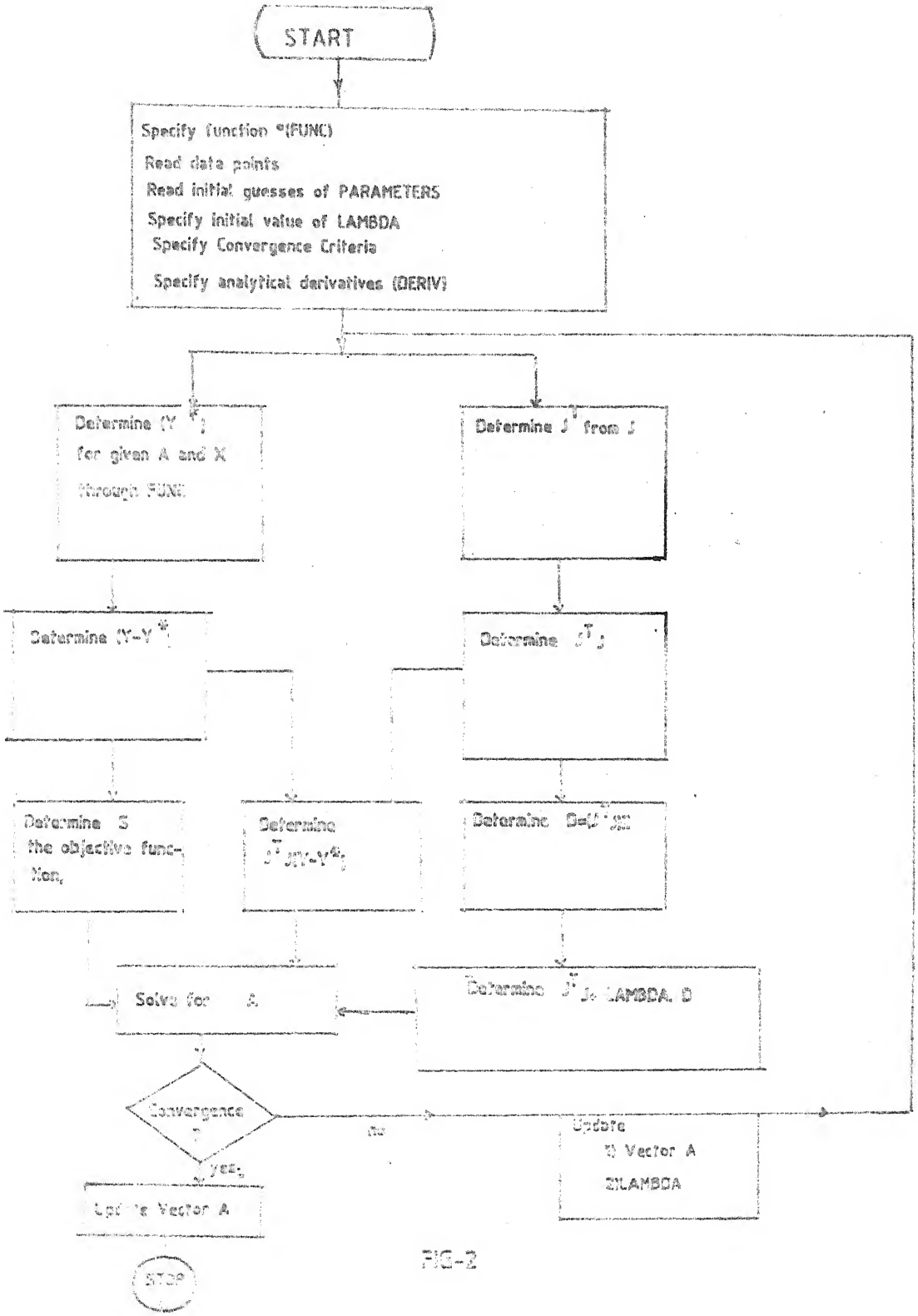
START
Specify function *(FUNC)
Read data points
Read initial guesses of PARAMETERS
Specify initial value of LAMBDA
Specify Convergence Criteria
Specify analytical derivatives (DERIV)
Determine (Y
for given A and X
through FUNC
Determine J^T from J
Determine (Y-Y*
Determine J^T J
Determine S
the objective func-
tion,
Determine
J^T (Y-Y*)
Determine De(J^T J)
Solve for A
Determine J^T J+ LAMBDA. D
Convergence
no
yes
Update
1) Vector A
2)LAMBDA
Update Vector A
STOP

FIG-2

if a parameter value was found to be negative it was reset to corresponding positive value before the start of subsequent iteration.

3.5 THE PROGRAM TO IMPLEMENT LEVENBERG-MARQUARDT'S ALGORITHM:

The program realising the chosen algorithm was developed as a part of the project. In order to be able to use the program on a routine basis, the program was made modular in nature. This ensures little overhead in changing the model, and the program is adequate for parameter extraction for the entire class of multivariable nonlinear equations. The changes called for are minimal. These are*

i) The dimension statement to be appropriately changed

ii) SUBROUTINE FUNC to be changed to incorporate the new model.

iii) SUBROUTINE DERIV - to be changed appropriately to analytical generate $\frac{\partial Y_i}{\partial A_J}$ / $J = 1, \ldots M$, $i = 1, \ldots N$

The flow chart of the program is given in Fig. 2, while the detailed algorithm is listed at Appendix B.

The results obtained and some of the peculiarities of the program are elaborated in the succeeding chapters.

CHAPTER 4

EXPERIMENTAL RESULT AND DISCUSSION

For a parameter extraction scheme like the one being followed there are three major requirements. These are

a) Model

b) Extraction algorithm

c) Experimental data

While requirements listed in (a) and (b) above have been discussed in the preceeding chapters, we will now examine the shape and form of experimental data to be provided as the third and final input to the scheme.

The triode region current-voltage relationship of N channel MOSFET (identical for P channel) is given by Eqn. (15), Chapter 2 which is rewritten here for convenience.

$$I_{ds} = K[\tfrac{4}{3} R(2\phi f)^{3/2}+(V_{GS}-V_{tx})V_{DS}-V_{DS}^{2}-4/3R(V_{DS}+2\phi f)^{3/2}] \quad (1)$$

In this equation, as it has been formed, I_{ds} the drain current is obviously the dependent variable. The independent variables are the gate to source voltage V_{GS} and the drain to source voltage V_{DS}. (It may however be

noted that the independent variable may change by rearranging the terms in a different form).

The Levenberg-Marquardt algorithm can take care of all the three variables (V_{GS}, V_{DS} and V_{BS}) at the same time. However it was decided to obtain data for I_{ds} vrs V_{DS} for constant V_{GS} because of the following reasons.

a) The I_{DS} vrs V_{DS} plot clearly exhibits the two distinct phase of operation; the triode region and the saturation region.

b) It is easy to graphically ascertain the pinch off voltage V_{sat}. once the parameters have been extracted, the accuracy of the parameters can be ascertained by calculating V_{sat} as per eqn. (16a) and (b) chapter 2.

c) It is easy to generate graphically the transfer characteristics of a CMOS, by having the I_{DS} vrs V_{DS} and I_{SD} vrs V_{SD} plot of the constituent N and P channel Mosfets. This transfer characteristics then in turn can be compared with numerically generated transfer characteristic (using extracted values of parameters) for point to point coincidence.

d) By keeping V_{GS} constant for a set of data the whole equation reduces to a simple one dependent and one independent variable. The analysis of the equation becomes easier.

Experimental Setup to Determine I-V Data for N Channel Mosfet(CD -4007)

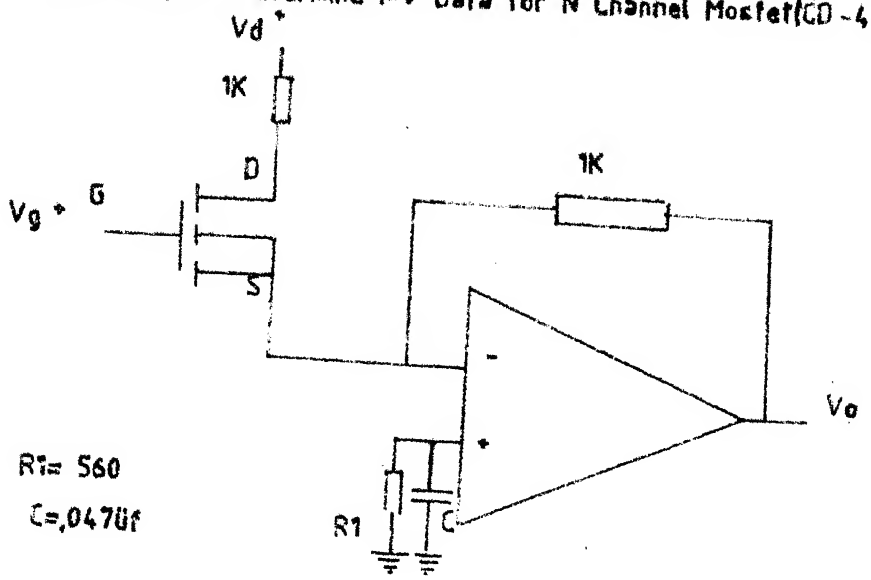

FIG- 3

Experimental Setup to Determine I-V Data for P Channel Mosfet (Cd-4007)

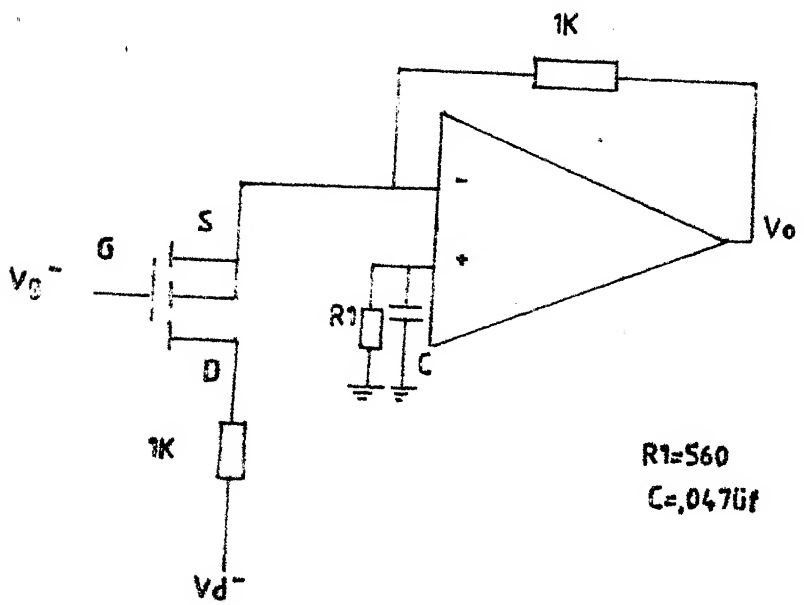

FIG- 4

4.1 EXPERIMENTAL ARRANGEMENT AND RESULTS:

a) N Channel Enhancement Mode MOSFET:

The scheme employed to determine the I_{DS} vrs V_{DS} data for the N channel MOSFET is shown in Fig. 3. A fixed bias was applied to the gate using a 12 bit DAC. The drain supply was connected through a current limiting resistor. The source was connected to the virtual ground of the opamp. The drain current was measured using an opamp as a CCVS. The voltage V_o is a measure of I_{DS} appropriately scaled. The voltage V_{GS}, V_{DS} and $V_o(I_{DS})$ were measured using a $6\frac{1}{2}$ bit digital multimeter. The data points thus determined are tabulated in Table 2.

b) P Channel:

The scheme for determining the data points of P channel is shown in Fig. 4 and is identical to the one used for N channel. Here too the source and substrate are internally connected and these in turn are connected to the virtual ground of the opamp. A negative voltage is applied to both source and drain. The data obtained is tabulated in Table 3.

The data that has been tabulated have been restricted to triode region of operation of both N and P channel Mosfets. Further as may be apparent from the two tables,

Table 2

SN	V_{GS}(v)	V_{DS}(v)	I_{DS}(ma)	SN	V_{GS}(v)	V_{DS}(v)	I_{DS}(ma)
1	4.2045	.1145	.1867	1	6.5015	.114	.3198
2	-do-	.224	.3466	2	-do-	.118	.3297
3	-do-	.322	.4745	3	-do-	.377	.9932
4	-do-	.439	.6098	4	-do-	.438	1.1382
5	-do-	.527	.6982	5	-do-	.588	1.4818
6	-do-	.637	.7925	6	-do-	.736	1.7967
7	-do-	.777	.8879	7	-do-	.843	2.0082
8	-do-	.814	.9097	8	-do-	1.010	2.314
9	-do-	.891	.9465	9	-do-	1.158	2.5585
10	-do-	1.020	.9912	10	-do-	1.326	2.8087
1	5.007	.0558	.1211	1	7.007	.126	.3764
2	-do-	.112	.2363	2	-do-	.266	.7697
3	-do-	.241	.4836	3	-do-	.492	1.3686
4	-do-	.396	.7538	4	-do-	.640	1.7301
5	-do-	.480	.8869	5	-do-	.837	2.180
6	-do-	.510	.9316	6	-do-	1.037	2.5932
7	-do-	.615	1.0816	7	-do-	1.184	2.8713
8	-do-	.730	1.2295	8	-do-	1.380	3.206
9	-do-	.807	1.3189	9	-do-	1.597	3.527
10	-do-	.933	1.4461	10	-do-	1.811	3.795
1	6.007	.1364	.3486	1	8.0026	.127	.4221
2	-do-	.206	.5104	2	-do-	.235	.7697
3	-do-	.397	.9514	3	-do-	.519	1.6258
4	-do-	.416	.9932	4	-do-	.698	2.1314
5	-do-	.570	1.3090	5	-do-	.910	2.6915
6	-do-	.632	1.4292	6	-do-	1.106	3.1723
7	-do-	.766	1.6735	7	-do-	1.353	3.7255
8	-do-	.850	1.8165	8	-do-	1.513	4.0483
9	-do-	.965	1.9993	9	-do-	1.755	4.4912
10	-do-	1.091	2.180	10	-do-	2.136	5.068

Table 3

SN	$V_{SG(v)}$	$V_{SD(v)}$	$I_{SD(ma)}$	SN	$V_{SG(v)}$	$V_{SD(v)}$	$I_{SD(ma)}$
1	4.003	.193	.2556	1	6.0067	.124	.255
2	-do-	.222	.2923	2	-do-	.172	.349
3	-do-	.464	.5747	3	-do-	.253	.5095
4	-do-	.645	.7620	4	-do-	.373	.744
5	-do-	.756	.8651	5	-do-	.495	.974
6	-do-	.934	1.0148	6	-do-	.617	1.199
7	-do-	1.188	1.1931	7	-do-	.650	1.256
8	-do-	1.204	1.2021	8	-do-	.823	1.562
9	-do-	1.262	1.2358	9	-do-	.943	1.765
10	-do-	1.362	1.2913	10	-do-	1.030	1.910
1	5.0030	.1392	.247	1	6.5015	.106	.230
2	-do-	.236	.407	2	-do-	.206	.4409
3	-do-	.366	.628	3	-do-	.309	.6604
4	-do-	.478	.806	4	-do-	.447	.9365
5	-do-	.557	.928	5	-do-	.623	1.2862
6	-do-	.673	1.102	6	-do-	.700	1.429
7	-do-	.756	1.221	7	-do-	.742	1.5126
8	-do-	.846	1.347	8	-do-	.888	1.785
9	-do-	.928	1.460	9	-do-	.892	1.814
10	-do-	1.290	1.913	10	-do-	1.225	2.381
1	5.5031	.148	.282	1	7.0031	.223	.501
2	-do-	.221	.418	2	-do-	.282	.626
3	-do-	.398	.736	3	-do-	.476	1.044
4	-do-	.462	.848	4	-do-	.554	1.205
5	-do-	.570	1.032	5	-do-	.736	1.579
6	-do-	.627	1.128	6	-do-	.913	1.936
7	-do-	.765	1.352	7	-do-	1.195	2.467
8	-do-	.853	1.4908	8	-do-	1.393	2.821
9	-do-	.984	1.690	9	-do-	1.430	2.888
10	-do-	1.444	2.331	10	-do-	1.462	2.942

the range of V_{GS}/V_{SG} has been restricted from 4v to 8v to obtain the data. The reasons for doing this are listed below.

i) For lower values of V_{GS} and V_{SG}, the range of V_{DS} and V_{SD} that define the triode region of operation for N and P channel transistors respectively, are greatly reduced, and the data points tend to get very close. Also the order of current being measured is less than .2 ma. Hence a small relative error in measurement reflects a large percentage error in data points. This may lead to erroneous values of parameters, when fed to the extraction program.

ii) For higher values of V_{GS} and V_{SG}, the currents I_{DS} and I_{SD} rise above 7.5 ma. This limit exceeds the manufacturers specification for both the IC and the opamp being used as a CCVS. Further the virtual ground of the opamp starts drifting, which will introduce error in data points.

Besides the data points, another input to the extraction algorithm are the initial guesses of the parameters being extracted. It was noted during program execution that for those functions where a unique solution to the parameter values were expected, the initial guess could be as wild as possible. The solution yielded was well within the acceptable error bound (less than .01%). However as has

been pointed out earlier in Chapter 3, the parameter extraction for Mosfets suffer from two potential sources of error namely,

a) The local minima

b) Redundancy/Insensitivity of the parameter.

While the local minima problem was easily resolved, the Redundancy problems demanded a fair initial guess. Fortunately device specifications were available which helped bring the initial guesses close to the expected values.

4.2 PARAMETER EXTRACTION:

a) For the test model:

To be able to verify the veracity of the program, a mathematical model, somewhat similar to J.E.Meyer's model for mosfet was employed. The mathematical model had five parameters, and a single independent variable. The data points were numerically generated. The output of the program is tabulated in Table 4.

From the table it is apparent that parameter A(1) is insensitive, and virtually remains unchanged. If this parameter's initial guess was changed to .99-1.01, it showed a tendency to stay there, thus yielding fruiteful results.

Table 4

SN	Parameters	Initial guess	Expected val.	Obtained val.	Least square error	Av. error/ data points
1.	A(1)	.90	1.0	.9047	.472 E-8	2.1E-5
2.	A(2)	2.2	2.0	1.981		
3.	A(3)	3.4	3.0	3.0036		
4.	A(4)	4.8	4.0	4.0073		
5.	A(5)	5.90	5.0	4.9996		

Another observation that was made during the parameter extraction of the mathematical model was that if the initial guesses were relaxed increasingly, a point was reached when the program showed a divergent tendency and showed no signs of turning in the correct direction even after 200 iterations.

Also in absence of any constraint on the parameters, the parameters A(1) and A(2) showed a trend to turn -ve, while the error minimisation was still being affected. This prompted an imposition of sign constraint in the algorithm, whereby if a parameter yielded at the end of an iteration was negative, it was reset to its corresponding positive value before entering the next iteration.

These lessons were noted and utilised for parameter extraction of Mosfets.

b) The MOSFET Parameter Extraction:

The Meyer's model focusses attention on three parameters. Having appropriately modified the subroutines 'FUNC' and 'DERIV' and substituted the test data with experimental data, the program was executed to yield the following results.

Table 5

4.2.b(i): N Channel

SN	V_{GS}	K		R		2Øf		Least Square objective Function	Average Error/Data point.
		INIT	EXT	INIT	EXT	INIT	EXT		
1.	4.2045	.309 E-3	.337 E-3	1.645	1.645	0.74	0.74	0.6795E-8	.255E-4
2.	5.007	-do-	.332 E-3	-do-	1.645	-do-	0.74	0.234E-8	.1554E-4
3.	6.007	-do-	.310 E-3	-do-	1.645	-do-	0.74	0.2166E-8	.149E-4
4.	6.5015	-do-	.299 E-3	-do-	1.645	-	-	0.7399 0.396E-8	.199E-4
5.	7.007	-do-	.287 E-3	-do-	1.6449	-		0.7398 0.159E-7	.399E-4
6.	8.0026	-do-	.270 E-3	-do-	1.6447	-		0.7386 0.2175E-7	.466E-4

4.2.b(ii): P Channel Table 6

SN	V_{SG}	K		R		2∅f		Least sq. objective Function	Average Error/Data Point
		INIT	EXT	INIT	EXT	INIT	EXT		
1.	4.0030	.189E-3	.240 E-3	0.78	0.779	0.62	0.6195	.245E-9	0.497E-5
2.	5.0039	-do-	.240 E-3	-do-	0.7794	-do-	0.6185	.190E-8	0.14E-4
3.	5.5031	-do-	.229 E-3	-do-	0.7788	-do-	0.6170	.387E-8	0.195E-4
4.	6.0014	-do-	.218 E-3	-do-	0.7795	-do-	0.6187	.111E-8	.11E-4
5.	6.5012	-do-	.209 E-3	-do-	0.7790	-do-	0.6177	.226E-8	.15E-4
6.	7.0047	-do-	.200 E-3	-do-	0.7709	-do-	0.5974	.542E-8	.238E-4

INIT = EXPECTED VAL/INITIAL VALUE

EXT = EXTRACTED VALUE

c) Use of 1/f noise for validation:

The theoretical expression relating the noise spectral power density with the device parameter [4] is given by

$$\frac{S_{ID}}{I_D^2} = \frac{K}{f^r} \quad \frac{Nt}{(C_{ox}+CD+C_{it}+\beta\mu_n)^2} \qquad (1)$$

with $K = \frac{q^4}{LZKT}$

for weak invenion $|\beta Q_n| \leq C_{ox} + C_D + C_{it}$ and

$$\frac{S_{ID}}{I_D^2} = \frac{K}{f^{\gamma}} \quad \frac{N_t}{(C_{ox}+C_D+C_{it})^2} \tag{2}$$

and for strong invenion $|\beta Q_n| >> C_{ox}+C_D+C_{it}$

$$\frac{S_{ID}}{I_D^2} = \frac{K}{f^{\gamma}} \quad \frac{N_t}{\beta^2 Q_n^2} \tag{3}$$

indicating that S_{ID}/I_D^2 strongly depends on gate bias through $1/Q_n^2$.

In the above three expressions

S_{ID} = current noise spectral power density

I_D = drain current

N_t = trap density ($ev^{-1}.cm^{-3}$)

= tunnelling const. for electron

β = q/kT

k = Boltzman's constant

q = electronic charge

T = absolute temperature

Q_n = channel charge

To validate the model and associated parameters the following steps could be employed.

1. Using Meyer's model (with the values of parameter extracted) $1/(\beta Q_n)^2$ can be calculated. This should have the same slope as S_{ID}/I_D^2. If this is true, value of $\frac{KN_t}{f^r}$ of eqn. (3) is known. If not the procedure has to be abandoned because N_t may be V_G dependent and this has to be experimentally determined first.
2. Use the value of $\frac{KN_t}{f^r}$ obtained to check the validity of eqn. (2), using C_{ox} and C_D as used in Meyer's model and ignoring C_{it}. If the experiment and theory agree, the effect of C_{it} is not important. otherwise methods have to be developed to include C_{it} in the model and use some other model than the one suggested by J.E. Meyer.

In the present work step (1) has been checked and the results are discussed below.

Fig. 5 shows the experimental set up used to determine S_{ID}/I_D^2. The results then obtained are tabulated in Table 7 and also plotted in Fig. 6.

EXPERIMENTAL SETUP FOR 1/f NOISE MEASUREMENT

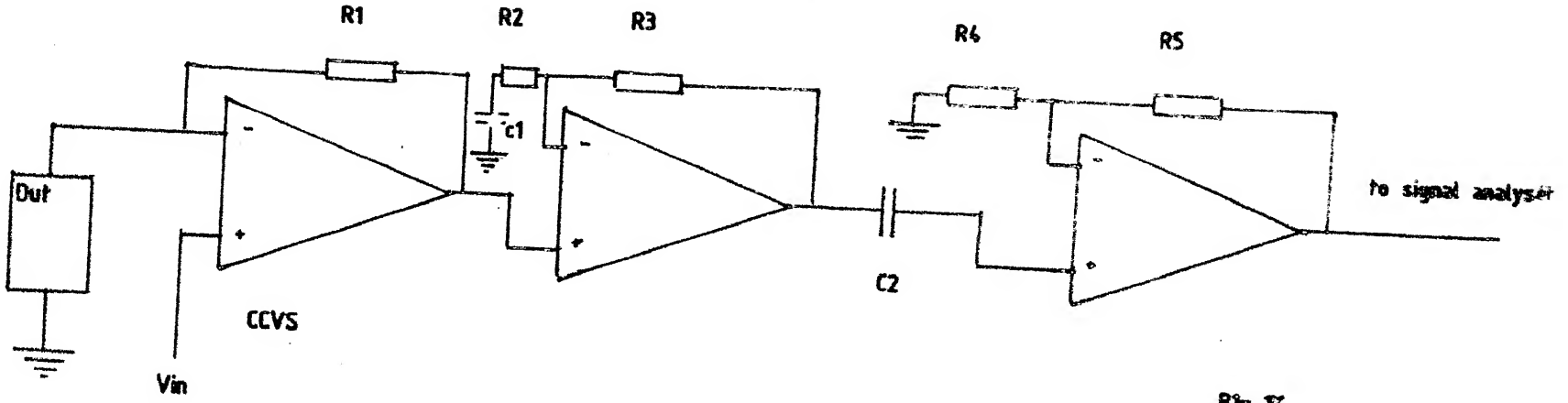

FIG-5

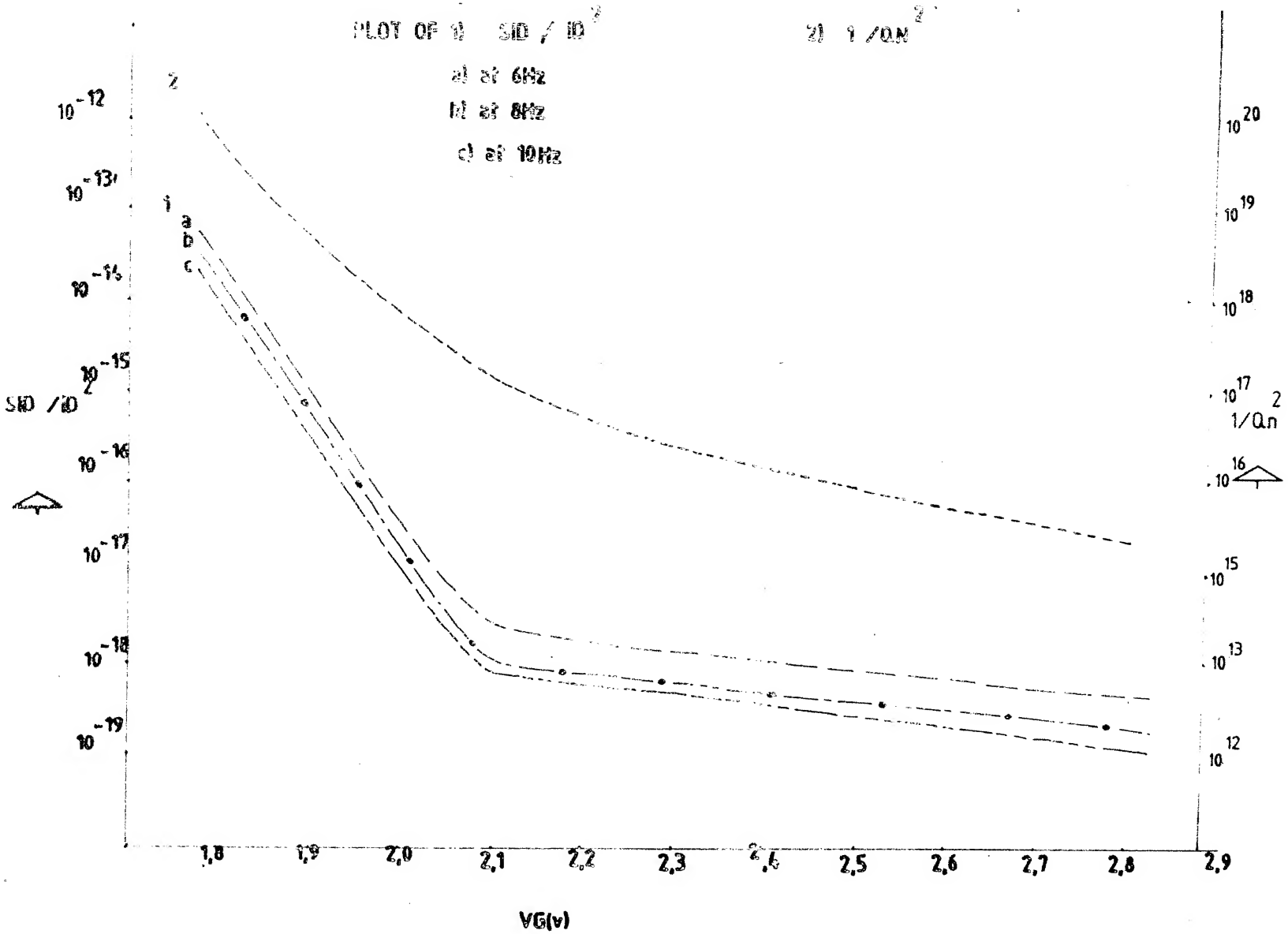
PLOT OF 1) SID / ID 2
2) 1 /Q.N 2
a) at 6Hz
b) at 8Hz
c) at 10Hz
1
2
a
b
c
10^{-12}
10^{-13}
10^{-14}
10^{-15}
10^{-16}
10^{-17}
10^{-18}
10^{-19}
SID /ID 2
10^{20}
10^{19}
10^{18}
10^{17}
10^{16}
10^{15}
10^{13}
10^{12}
2
1/Q.n
1,8
1,9
2,0
2,1
2,2
2,3
2,4
2,5
2,6
2,7
2,8
2,9
VG(v)

FIG— 6

42

Table 7

V_D = .5V

SN	V_G	Frequency	$A^2/Hz.$ S_{ID}/I_D^2	SN	V_G	Frequency	S_{ID}/I_D^2
1	1.867	6	4.845E-14	7	2.4169	6	1.50E-18
		8	2.688E-14			8	7.48E-19
		10	1.467E-14			10	5.85E-19
2	1.8759	6	6.8889E-14	8	2.6062	6	8.157E-19
		8	3.448E-14			8	4.176E-19
		10	2.405E-14			10	3.161E-19
3	1.9150	6	1.371E-14	9	2.9248	6	4.87E-19
		8	8.76E-15			8	1.756E-19
		10	7.228E-15			10	9.34E-20
4	1.9911	6	3.96E-15				
		8	3.109E-15				
		10	2.275E-15				
5	2.1069	6	3.588E-15				
		8	2.359E-15				
		10	1.873E-15				
6	2.2192	6	2.204E-18				
		8	9.528E-19				
		10	7.83E-19				

For strong invenion as has been brought out earlier

$$\frac{S_{ID}}{I_D^2} = \frac{K}{f^r} \quad \frac{N_t}{\beta^2 Q_n^2} \tag{4}$$

A plot of $1/Q_n^2$ against V_G has been taken and is shown in Fig. 6.

To determine Q_n an approximation has been made

$$I_D = \frac{\mu Z}{L} \; Q_n(V_G) V_D \tag{5}$$

for small values of V_D.

The term μ refers to effective mobility and its value has been taken from the value of K extracted, using Levenberg-Marquardt.

On comparing the curves $\frac{S_{ID}}{I_D^2}$ vrs V_G and $\frac{1}{Q_n^2}$ vrs V_G, we find that the two are nearly parallel, and indicating that N_t is at best weakly dependent on V_G. The constant $\frac{KN_t}{f^r}$ thus obtained for various values of V_G are tabulated in Table 8.

In order to check step (2), I_D in weak inversion region (order na amps) has to be measured. This could not be performed due to the inability of present setup used in the experiment. However it was found that the current spectral power densities are well defined in subthreshold biases too.

Table 8

f	V_G	$\frac{KN_t}{f^r}$ (coulomb^2 volt^2 sec)
6 Hz	1.875	$.2943 \times 10^{-34}$
	1.9150	$.2749 \times 10^{-36}$
	1.9911	$.6990 \times 10^{-36}$
	2.1069	$.2949 \times 10^{-35}$
	2.2192	$.924 \times 10^{-38}$

4.2.2 Some Comments on the Extraction Algorithm Behaviour relevent to Model under Study:

Some of the common tendencies of the extraction algorithm noted are elaborated below.

a) Susceptability to initial guess:

Of three parameters K,R and $2\phi f$, the parameter R and $2\phi f$ were mostly insensitive during least square error minimisation. The values of these parameters obtained on convergence showed an affinity to the initial guesses provided for these. If the initial guess for these parameters

was relaxed continuously, the extraction algorithm tended to diverge.

(b) Sensitivity of the parameter:

Of the three parameter the parameter K was most sensitive and showed scant respect for its initial guess. The remaining two parameters were in comparision, insensitive

(c) Constrained Minimisation:

In absence of any constraint on the parameters the program often tended to yield negative values for K and R while the least square minimisation was still being achieved. In order to obtain the correct sign and values of parameters a constraint was imposed on the sign of the parameters. This helped bring the program execution to order.

(d) Choice of Mathematical Function:

All the above tendencies were found absent, when the extraction algorithm was extended to a well defined mathematical function, where all parameters were independent and unique in their values. The extraction algorithm always yielded results with an accuracy better than .01% and took fewer iterations to converge.

Hence it may be worthwhile to select those models where parameters are well defined, independent and unique. However this may not always be possible.

4.3 THE MOBILITY BEHAVIOUR:

As expected the parameter K for both N and P channel show a decline with increasing value of V_{GS} and V_{SG} as expected because the parameter

$$K = \frac{\mu E_{ox} W}{2LT_{ox}}$$

The term μ refers to effective mobility and as anticipated it shows a degradation with increasing gate bias. The graph showing the mobility behaviour of N and P channel as extracted from the parameters yielded by Levenberg-Marquardt's algorithm are plotted in Fig. 7.

Using equation for mobility

$$\mu_{eff} = \mu_{eff(o)} \left(\frac{E_{so}}{E_s} \right)^q \qquad (6)$$

where $E_{so} = 6 \times 10^4$ v/cm

$$E_s = (V_{GS} - V_{tx} - 0.5 \text{ vds})/T_{ox}$$

an attempt was made to calculate the value of 'q' the mobility degradation factor. It was observed that value of q thus obtained showed a wide dispersal rather than being a constant as expected.

PLOT INDICATING MOBILITY DEGRADATION

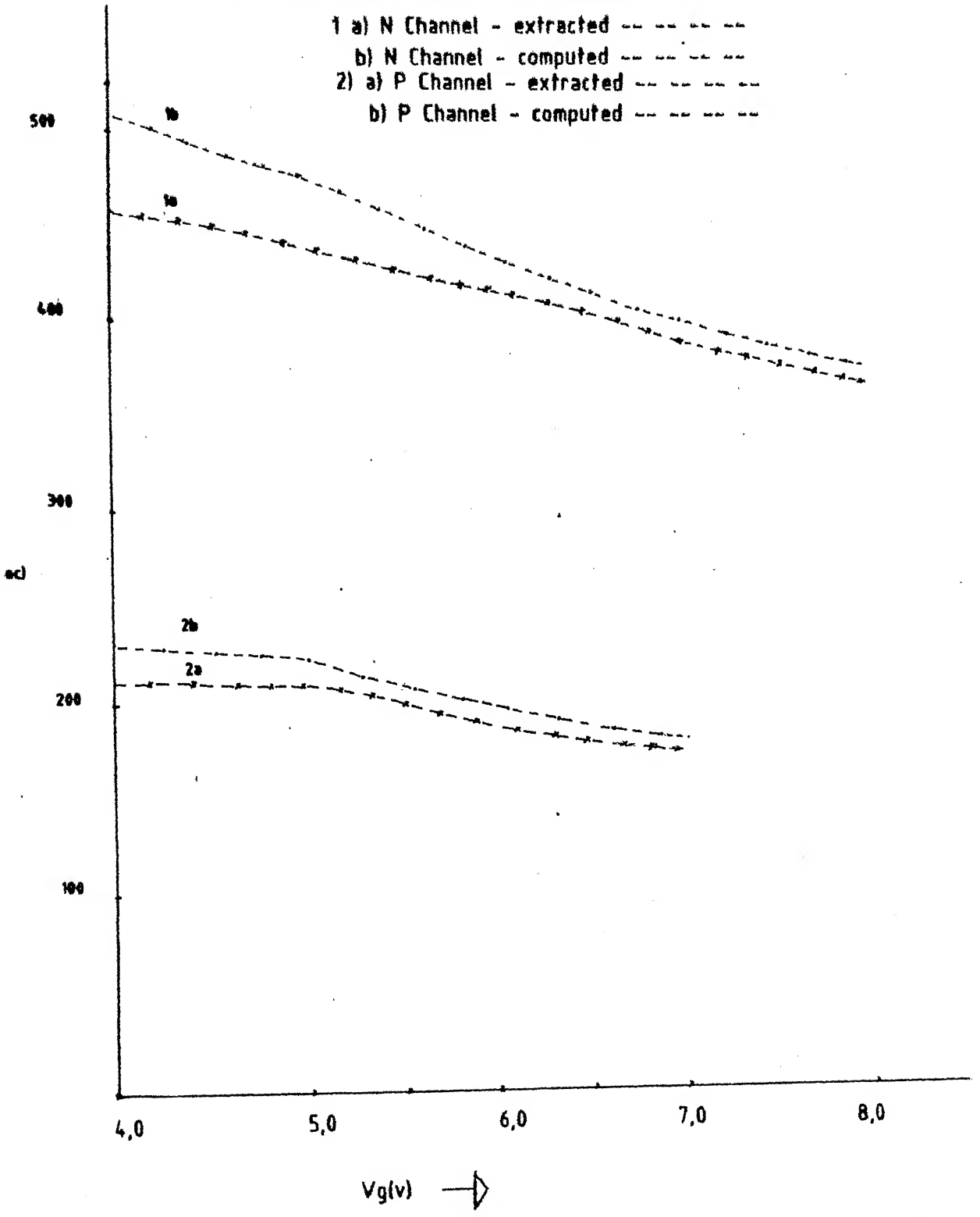

FIG-7

Therefore an effort was made to go in for newer model, which could explain the observed mobility behaviour. It was found that the imperical model proposed by S.C. Sun and James Plummer [7] explained the observed mobility phenomenon with a fair degree of accuracy.

The model proposed aims to derive effective mobility from d.c. drain conductance gd. The effective mobility is related to the drain conductance by (refer Fig. 8).

$$\mu_{eff} = \frac{(L/W)gd}{q\ N_{inv}} \Big/ VD \quad 0 \qquad (7)$$

with

$$q\ N_{inv} = C_{ox}\ \ V_G - V_T - \frac{1}{2}\left[1 + \frac{a}{2\sqrt{2}\ \ln\ \ N_A/N_i}\right].VD \qquad (8)$$

and $a = \sqrt{2}\ (\ _{si}t_{ox}/\ \ _{ox}\ L_B)$

and L_B the Bulk Debye length

$$= \sqrt{\left(\frac{KT}{q}\ \ \frac{E_{Si}}{q\ N_A}\right)} \qquad (9)$$

From the device specifications provided, in conjunction with the experimental data, μ_{eff} was computed for both N and P channel. The results are tabulated in Tables 8 and 9, and also plotted in Fig. 7 .

RELATION BETWEEN EFFECTIVE MOBILITY AND FIELD EFFECT MOBILITY

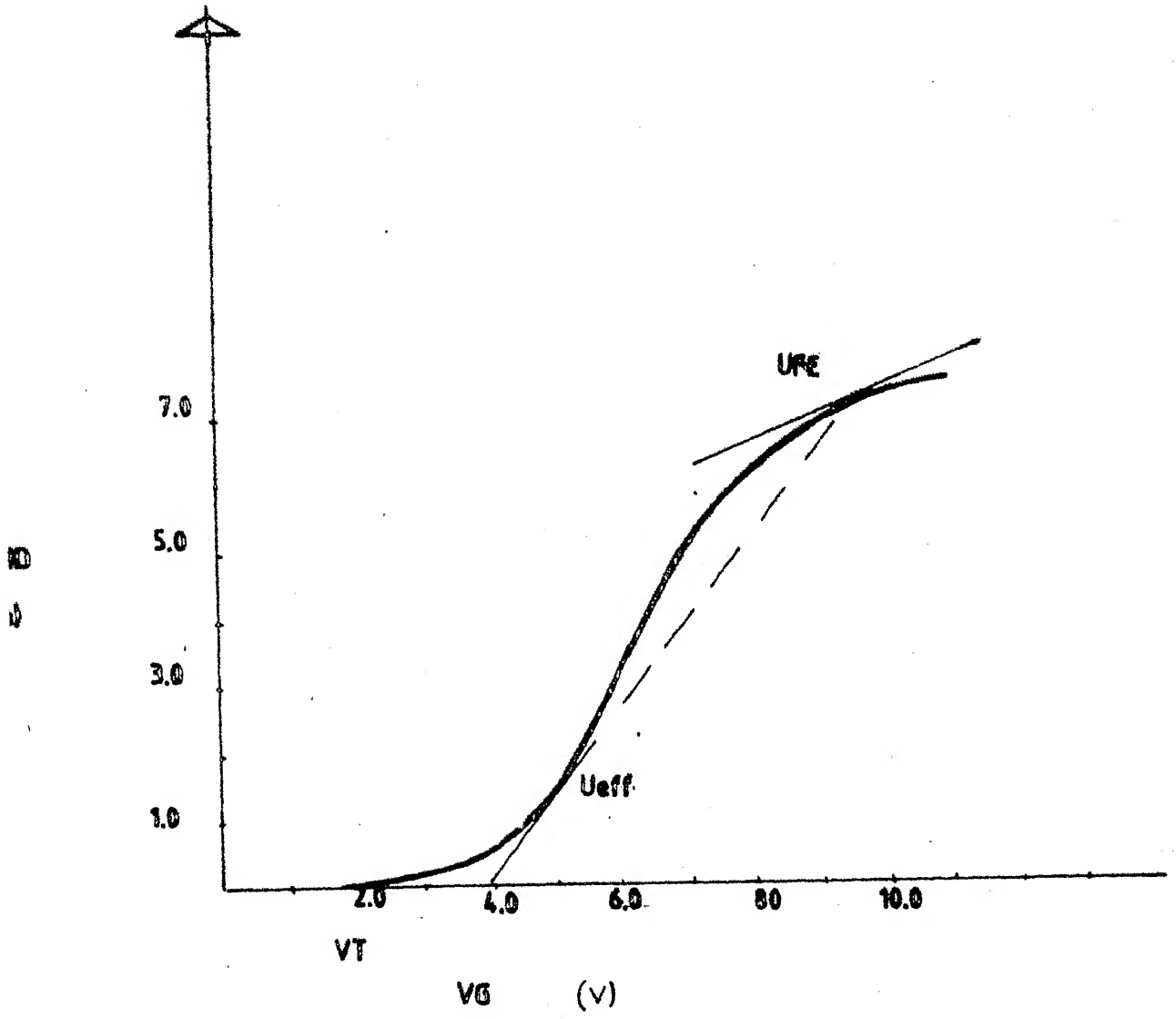

FIG-8

Table 8

N Channel

SN	V_G	G_d at V_D (mho)	L/W gd (mho)	q_{Ninv} at V_T= 1.85	μ_{eff} (cm^2/V sec.)
1	4.2045	$1.6305\times10^{-3}/V_D=.1145$	$.326\times10^{-4}$	$.0645\times10^{-6}$	505.4
2	5.007	$2.1702\times10^{-3}/V_D=.0558$	$.434\times10^{-4}$	$.0907\times10^{-6}$	478.5
3	6.007	$2.555\times10^{-3}/V_D=.1364$	$.511\times10^{-4}$	$.1165\times10^{-6}$	437.87
4	6.5015	$2.8052\times10^{-3}/V_D=.114$	$.561\times10^{-4}$	$.1323\times10^{-6}$	424.0362
5	7.007	$2.9873\times10^{-3}/V_D=.126$	$.597\times10^{-4}$	$.1467\times10^{-6}$	406.95
6	8.0026	$3.323\times10^{-3}/V_D=.127$	$.664\times10^{-4}$	$.1760\times10^{-6}$	377.272

Table 9

P Channel

SN	V_G	G_d at V_D (mho)	L/W gd (mho)	q_{Ninv}	μ_{eff} cm^2/V sec.
1	4.003	$1.324\times10^{-3}/V_D=.193v$	$.0169\times10^{-3}$	$.0720\times10^{-6}$	234.72
2	5.0030	$1.774\times10^{-3}/V_D=.1392v$	$.02274\times10^{-3}$	$.1028\times10^{-6}$	221.20
3	5.5031	$1.905\times10^{-3}/V_D=.148v$	$.02442\times10^{-3}$	$.1173\times10^{-6}$	208.184
4	6.0067	$2.056\times10^{-3}/V_D=.124$	$.02635\times10^{-3}$	$.1328\times10^{-6}$	198.41
5	6.5015	$2.169\times10^{-3}/V_D=.106$	$.02780\times10^{-3}$	$.1478\times10^{-6}$	188.09
6	7.0031	$2.2466\times10^{-3}/V_D=.223$	$.02880\times10^{-3}$	$.1597\times10^{-6}$	180.338

It should be noted that the effective mobility is distinct from the field effect mobility μ_{FE}, which is obtained from the transconductance g_m and is defined by

$$\mu_{FE} = \frac{(L/W)}{C_{ox}V_D} \left(\frac{d_{ID}}{d_{VG}}\right)/V_D \quad O \qquad (10)$$

The relationship between the effective mobility and field effect mobility is also shown in Fig. 8. It is apparent that the mobility data from g_d and g_m measurements are essentially identical at the point of maximum slope (near V_T). Beyond the point of inflection, the field effect mobility is always smallert than the effective mobility. Therefore if μ_{FE} is used in device modelling currents and device switching speeds will be under estimated.

4.4 VALIDATION OF EXTRACTED PARAMETERS:

The question that readily comes to ones attention is how good are the parameters extracted? Are the parameters extracted capable of simulating the device behaviour in the entire region of operation and if so, then with what degree of accuracy? Do also the parameters extracted have a well defined physical significance.

To put these doubts to rest, the extracted parameters were subjected to a variety of validation schemes. The schemes employed are

I – V DATA N CHANNEL

a)Experimental

b)Simulated

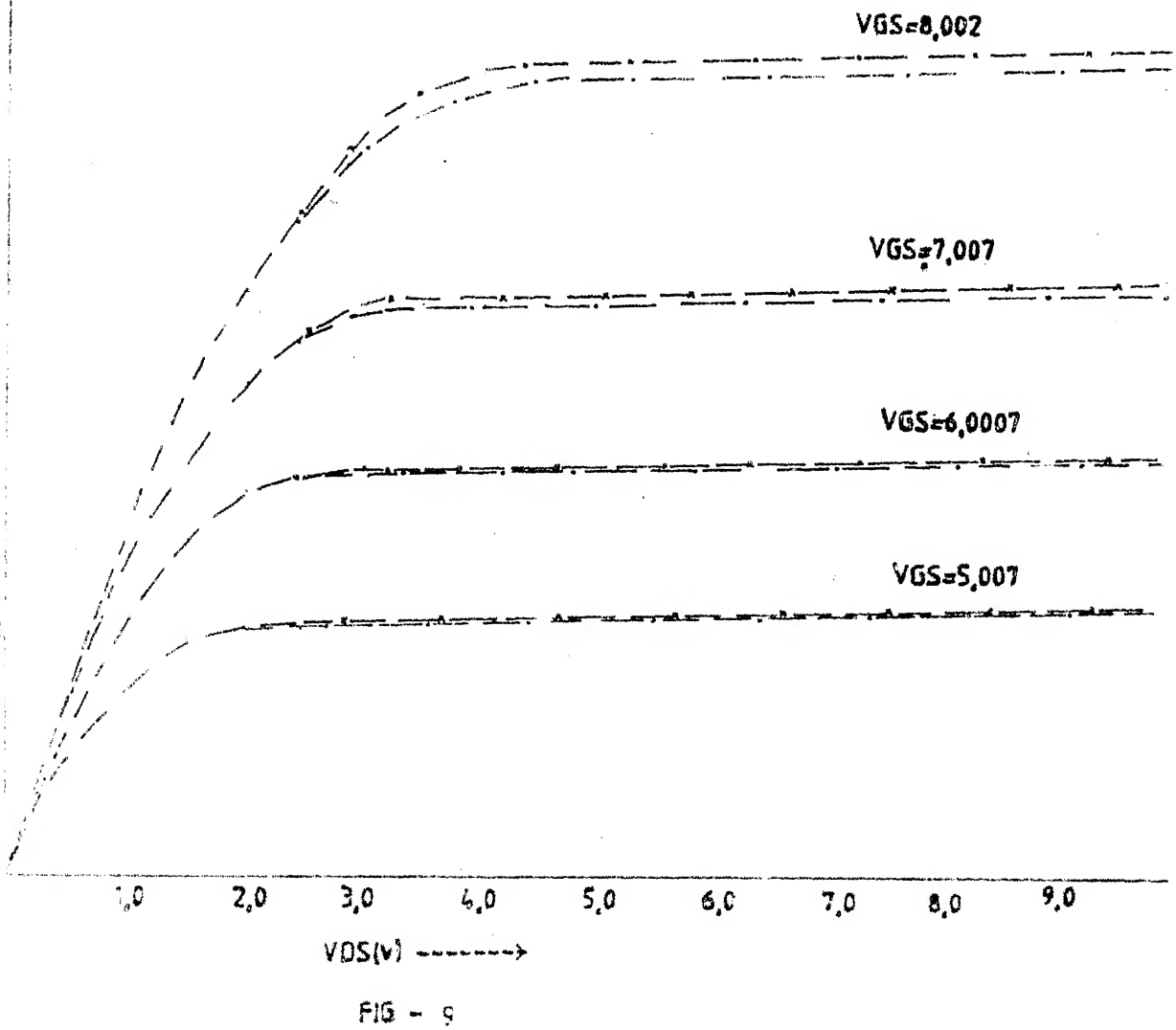

FIG – 9

I–V DATA P CHANNEL (CD 4007)

a) Experimental

b) Simulated

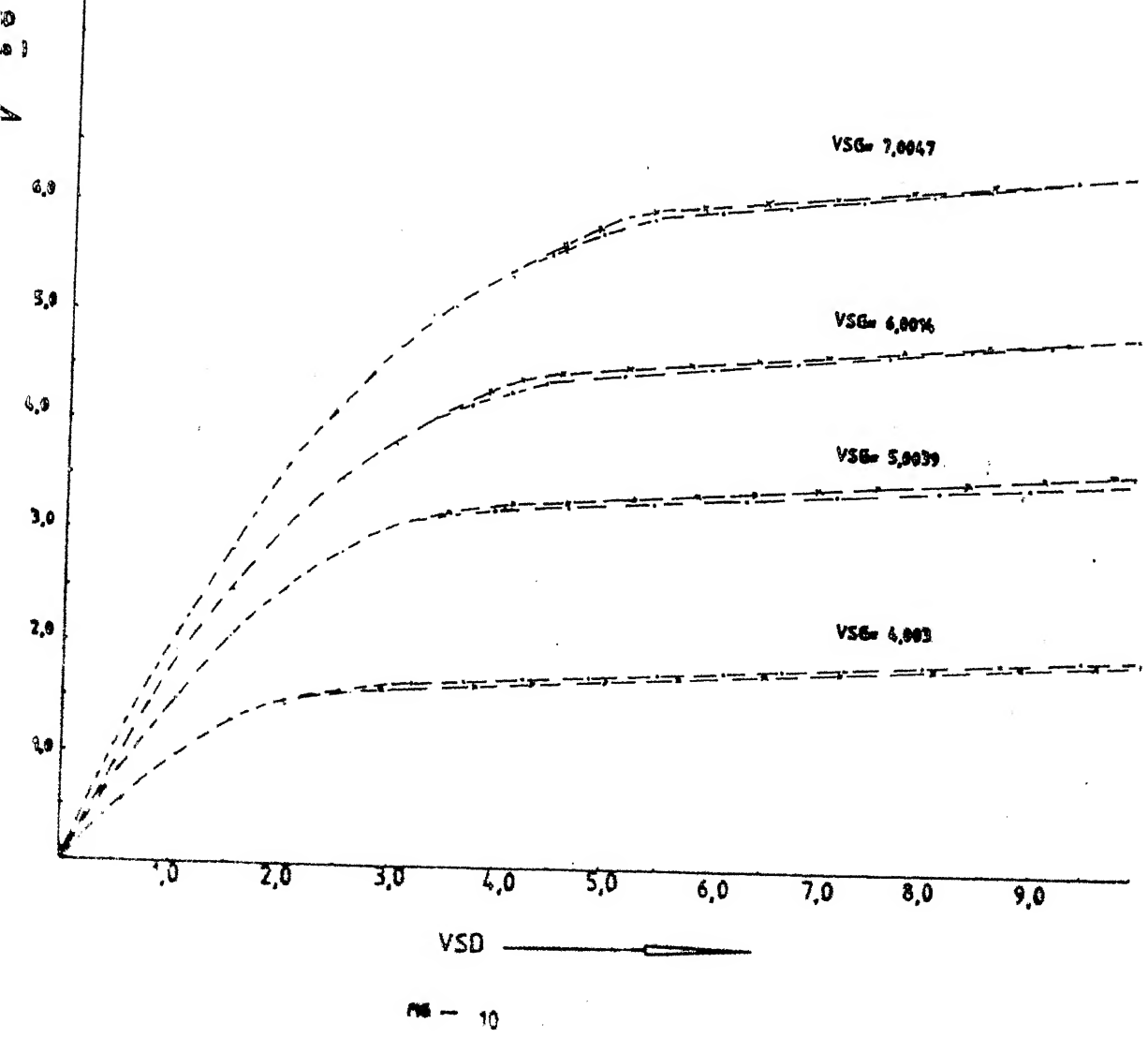

FIG — 10

a) simulation of dc characteristics for the N and P channel MOSFETS and a comparison with experimental I-V characteristics.

b) Simulation of transfer characteristics of CMOS inverter comprising of the N and P channel MOSFETS under study, and comparing it with experimentally obtained transfer characteristics.

4.4(a): Simulation of d.c. Characteristics:

The I-V characteristics of N and P channel have been simulated using extracted value of parameters. The two plots, experimental and simulated are illustrated in Fig. 9 for N channel and 10 for P channel. They show a fair coincidence for both N and P channel.

It may be argued that such a validation scheme is superflours, since the data point for extraction algorithm using least square minimisation have been provided from the experimental I-V graph, and that coincidence is only expected since convergence criteria has been satisfied.

As a matter of fact, it is not so. The data points for extraction algorithm have been chosen from a limited range of device operation namely the triode region. Here the simulation is being attempted for both the triode and

saturation region. The most critical area of curve fitting is the 'Knee' or the pinchoff voltage referred in this thesis as V_{sat}.

It was pointed out earlier that in the I-V relationship proposed by J.E. Meyer, two of the parameters R and 2Øf were found rather insensitive, despite the fact that least square minimisation was being achieved. These two parameters tended to track the initial guess.

However these parameters are dominant in determining the 'Knee', as such there may arise a requirement for upgrading the initial guesses for these parameters to obtain the best fit concurrently satisfying the convergence criteria of the extraction algorithm. The fact that such a curve fitting has been obtained, helps buildup a confidence towards the values of the parameters extracted.

4.4(b): Simulation of Transfer characteristics of the CMOS Comprising of N and P channel Mosfets:

This scheme in essence is a further enhancement of the previous scheme. Here the aim is to check the behaviour of the two transistor while interacting with each other. The flow chart of the algorithm followed is at Appendix C. Also refer to Fig. 11 for the configuration in which the two MOSFETS are arranged.

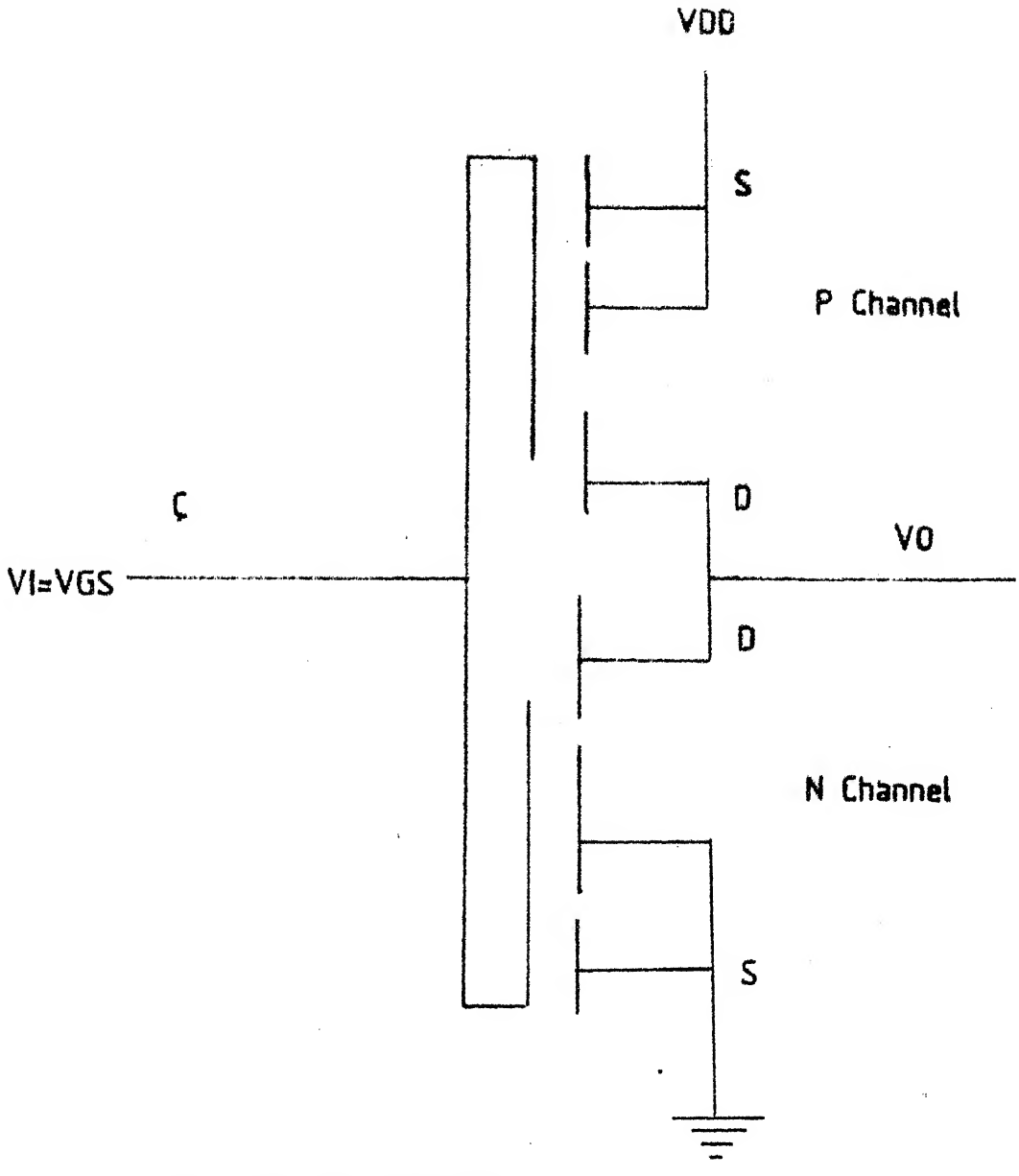

CRITERIA FOR CMOS OPERATION

a) Ids (N Channel)= Isd (P Channel)

b) vi=VGS (N channel) and VSG (P channel)= VDD-Vi

c) VDS (N Channel)=VO and V_{SD} (P Channel)=VDD-VO

FIG-11

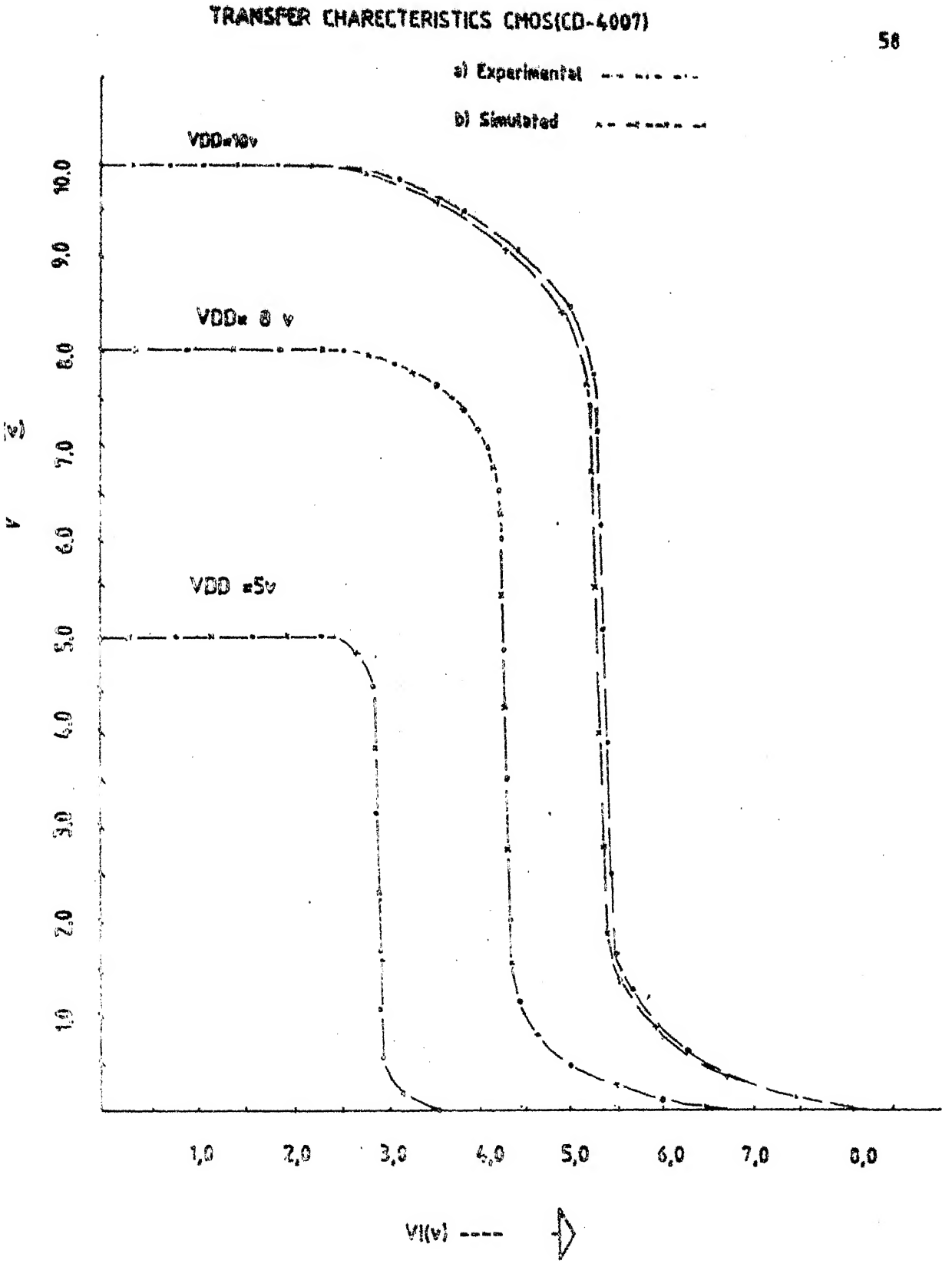
TRANSFER CHARECTERISTICS CMOS(CD-4007)
a) Experimental
b) Simulated
VDD=10v
VDD= 8 v
VDD =5v
10.0
9.0
8.0
7.0
6.0
5.0
4.0
3.0
2.0
1.0
V
0
1,0
2,0
3,0
4,0
5,0
6,0
7,0
8,0
VI(v) ----

FIG - 12

The simulated transfer characteristics and experimental transfer characteristics are plotted in Fig. 12. Good point to point coincidence is obtained between the two plots thereby further validating the parameter values.

4.4 ERROR ANALYSIS:

While care has been taken to minimise error at all stage, it is not possible to completely eliminate the error. There are several potential sources of error and these must be identified to decide on the error tolerance of the result. These sources of error are

a) Accuracy of the model

b) Measurement inaccuracies

c) Convergence criteria used for extraction algorithm

d) Instrumentation error

4.4(a) Accuracy of the Model:

The triode region behaviour of the MOSFETS have been found to,be adequately well explained by the Meyer's model. However the linearisation of the model in saturation region is not accurate and has a inbuilt source of error. The model is specially vulnerable at pinch off, when the device operation makes a transition from triode to saturation region. While the experimental I-V data is smooth over the

entire range of operation, the Meyer's model induces an abrupt jump in current value at pinch off.

4.4(b): Measurement inaccuracies:

An opamp based CCVS has been employed. The leakage current of the opamp, though of the order of na have been ignored. Further the offset voltage tended to increase with increasing value of current. This is bound to introduce error, which may not be very significant if proper care is taken during measurements.

4.4(c): Convergence criteria used for Extraction Algorithm:

Fairly stringent convergence criteria has been used in this case, but it is by no means zero as is to be expected. This may lead to a very small error. An attempt to further minimise the error needs far greater computation time.

4.4(d): Instrumentation Error:

The device used for measurement of all voltages is the $6\frac{1}{2}$ digit multimeter. It was found that if different multimeter scales were used to measure the same data, it showed a departure which was scale dependent. To minimise the error, the entire set of data points were taken on the same scale.

CHAPTER 5

CONCLUSION

Computer aided simulation is finding tremendous favour with manufacturers and users of LSI and VLSI chips. To be able to simulate the device behaviour, accurate device parameters as also the domain of operation (external variables) are the major ingredients

In this project CMOS CD4007 has been studied in d.c. operation and related parameters have been extracted. For extraction of parameters Levenberg-Marquardt's algorithm has been developed and implemented using experimental I-V data points in the triode region. The program developed is modular in nature and can be extended to any model function having multiple parameter, with minimal changes.

The values of parameters have been checked by a number of schemes. These are:

a) Simulation of I-V characteristics of N and P channel mosfet.

b) Simulation of CMOS transfer characteristic comprising of the two transistors.

c) Mobility analysis

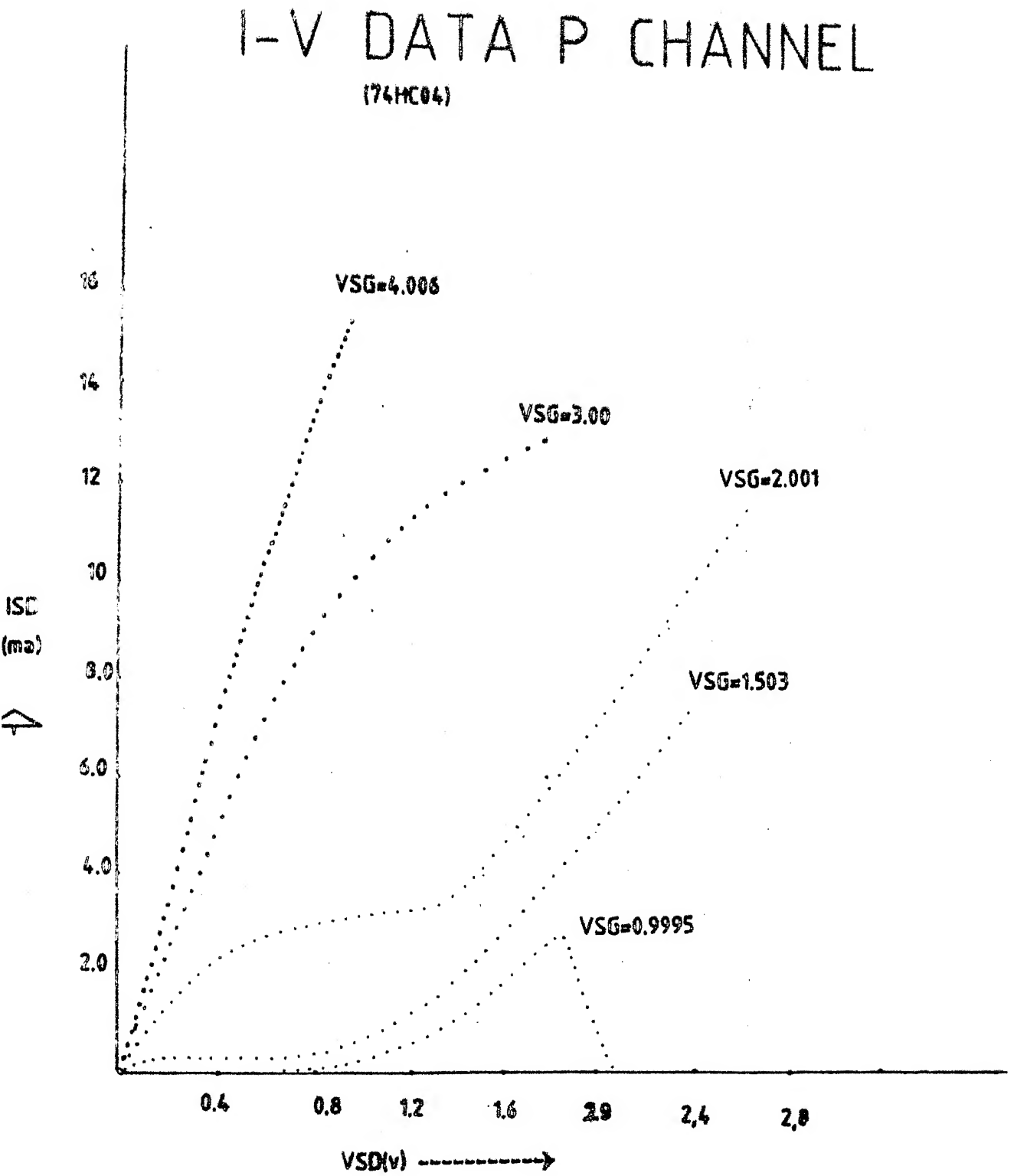
I-V DATA P CHANNEL
(74HC04)
VSG=4.006
VSG=3.00
VSG=2.001
VSG=1.503
VSG=0.9995
16
14
12
10
8.0
6.0
4.0
2.0
ISD
(ma)
0.4
0.8
1.2
1.6
2.0
2,4
2,8
VSD(v)

FIG-13

The parameters values obtained show satisfactory results as proved by a number of validation schemes employed.

Error analysis has been made, and also comments on the peculiarities of extraction algorithm under certain conditions has been described. Some data has also been taken on 1/f spectral power density of N channel MOSFETS.

5.1 SUGGESTIONS FOR FURTHER WORK:

a) Initially the device chosen was 74HC04. The I-V characteristics(refer Fig.13) of this high speed CMOS were found very different from that of normal CMOS 74C04, CD4007. Meyer's model was found wanting in explaining the phenomenon observed. A search for a model that can describe the I-V characteristics of 74HC04 can be carried out, and its parameter extracted. The I-V data for 74HC04 has been plotted in Fig.13 for ready reference.

b) The device under study does not provide for studying the effect of source to substrate bias. Since Meyer's model explains the effect of source to substrate bias, those N and P channel device (MFE 3001, MFE 3003 respectively) could be chosen which facilitate the application of source to substrate bias, and its behaviour studied.

c) Observations were also made to determine the values of C_{ox}, using a C-V plotter. It was found that the

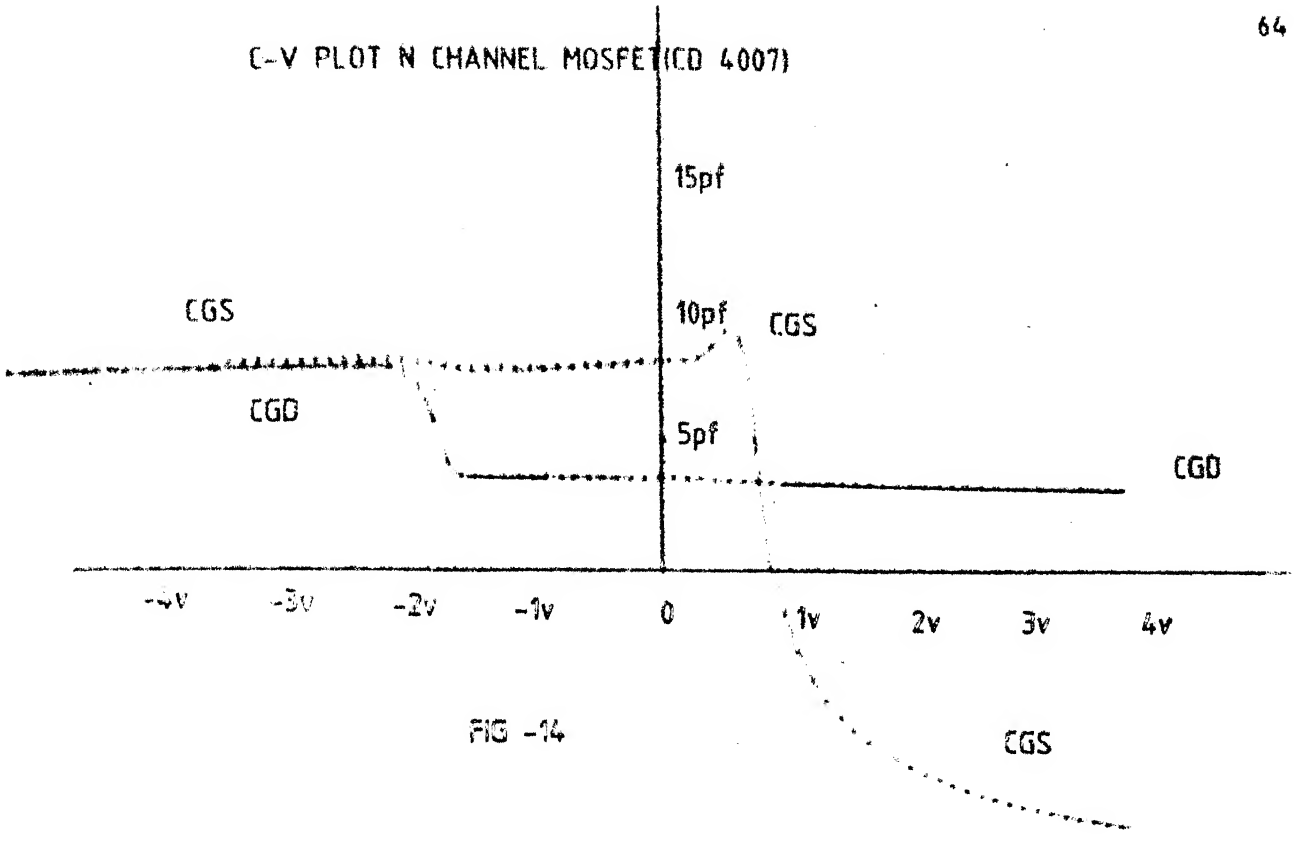
C-V PLOT N CHANNEL MOSFET(CD 4007)
15pf
10pf
5pf
CGS
CGD
CGS
CGD
-4v
-3v
-2v
-1v
0
1v
2v
3v
4v
CGS

FIG -14

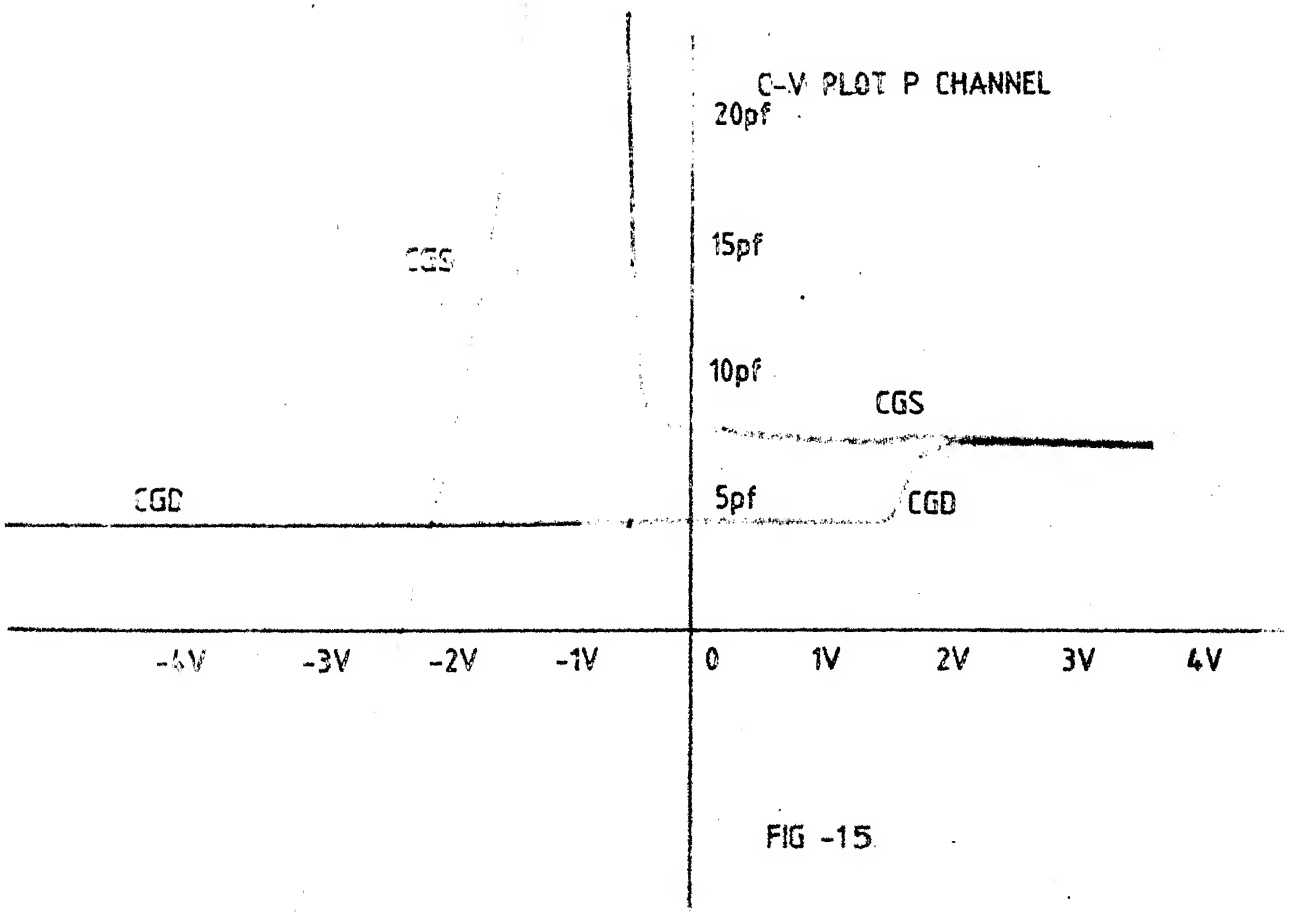
C-V PLOT P CHANNEL
20pf
15pf
10pf
5pf
CGS
CGS
CGD
CGD
-4V
-3V
-2V
-1V
0
1V
2V
3V
4V

FIG -15

transition capacitance of the protective zenner completely masked the values of CGS and CGD . Meyer's model of voltage dependent capacitances finds favour with latest simulation programme like SPICE1 and SPICE2, hence the same may be analysed using N and P channel mosfet that have no zenner protection; as it would help throwup information about fast surface state densities. The C-V data taken for N and P channel are shown in Figs. 14 and 15 respectively. The value for C_{ox} for N channel MOSFET expected is in the vicinity of 0.2 pf and that of P channel MOSFET is in the vicinity of .14 pf.

d) In the noise measurement scheme data has been taken for only the strong inversion case. The weak inversion case involves measurement of subthreshold current measurements which are of the order of nA and less. An electrometer may be employed to get S_{ID}/I_D^2 for weak inversion region.

There are many more facets of the device that one could be interested in, but it is hoped that the above suggestions if implemented may just about roundup the d.c. and noise behaviour of the device under study.

APPENDIX A

DEVICE PHYSICS CONCEPT REVISITED

The most important parameter in semiconductor physics is the band gap E_g which separates the lowest energy state in the conduction band from the highest energy state in the valence band.

For a intrinsic semiconductor the number of occupied conduction band level is given by

$$n = \int_{E_c}^{E_{top}} N(E)F(E)dE \qquad (1)$$

where

E_c = energy at the bottom of conduction band

E_{top} = energy at the top of conduction band

$N(E)$ = density of states

$F(E)$ = The Fermi-Dirac distribution function given by

$$F(E) = \frac{}{1+\exp(\frac{E-E_F}{KT})} \qquad (2)$$

where

K = Boltzman's constant

T = absolute temperature

E_F = Fermi potential

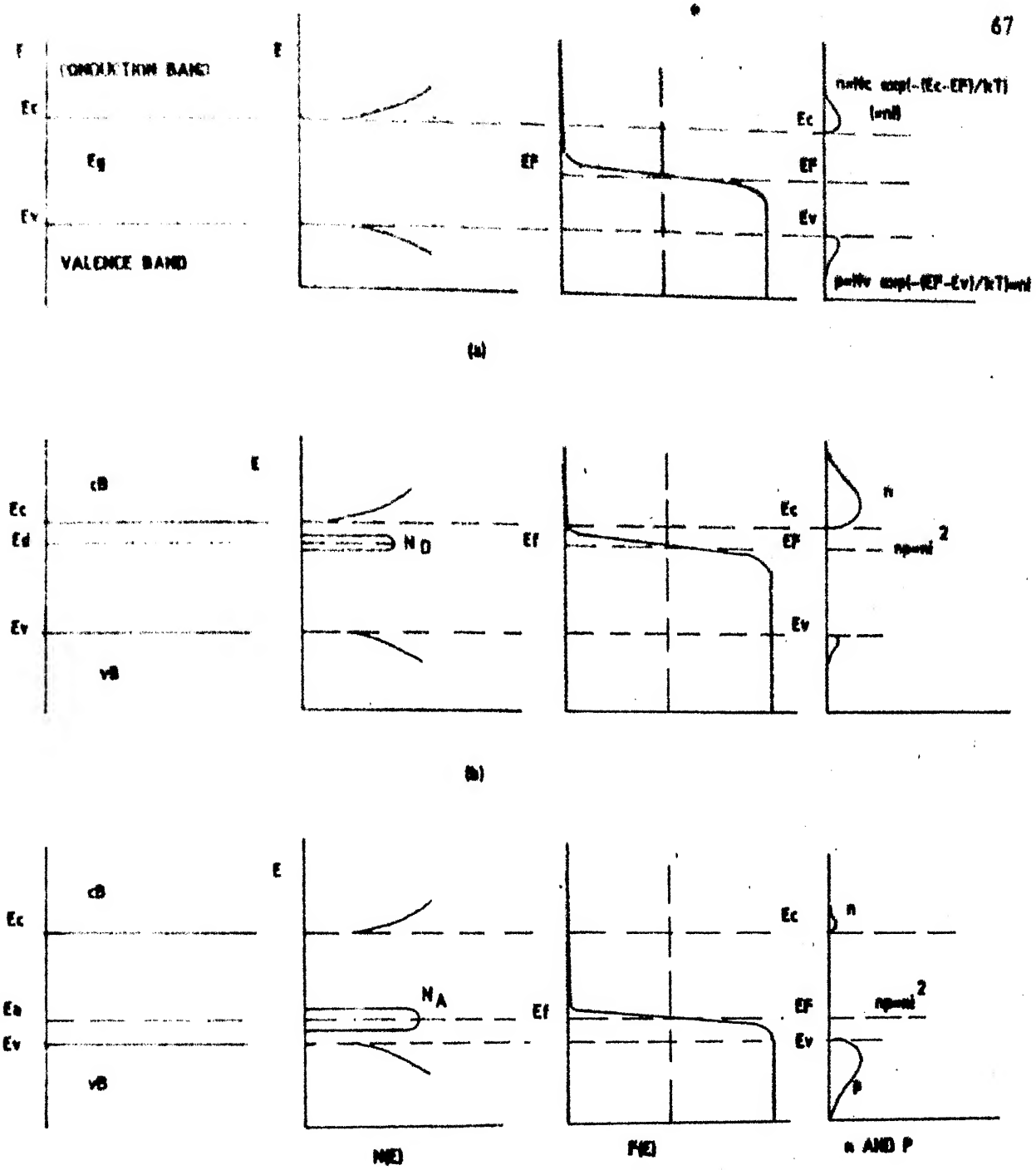

Schematic band diagram, density of states, Fermi-Dirac distribution, and the carrier concentrati

-on for a)intrinsic semiconductor

b)N-type semiconductor

c)P-type semiconductor

FIG- 16

From equations (1) and (2) we have

$$n = N_c \exp\left(-\frac{E_c - E_F}{KT}\right) \qquad (3)$$

where N_c is the effective density of states in the conduction band.

Similarly the hole density near the top of the valence band is given by

$$p = N_v \exp\left(\frac{-E_F - E_v}{KT}\right) \qquad (4)$$

Also, the Fermi level E_F for the intrinsic semiconductor is given by

$$E_F = E_i = \frac{E_c + E_v}{2} + \frac{KT}{2} \ln\left(\frac{N_v}{N_c}\right) \qquad (5)$$

Hence the Fermilevel E_F for the intrinsic semiconductor lies very close to the middle of the band gap. Refer Fig.16(a).

The intrinsic carrier density is obtained by

$$n.p = n_i^2 = N_c N_v \exp\left(-\frac{E_g}{KT}\right) \qquad (6)$$

when impurity are introduced, the Fermi-level must adjust itself to preserve charge neutrality. Consider the case shown in Fig.16(b) where donor impurities with concentration $N_D(cm^{-3})$ are added to the crystal. To preserve the electrical

neutrality the total negative charges (electron and ionised acceptors) must equal the total positive charges (holes and ionised donors) or

$$n = N_D^+ + p \qquad (7)$$

where

n = electron density in the conduction band

p = holes density in the valence band

N_D^+ = the no. of ionised donors

$$N_D^+ = N_D \left[1 - \frac{1}{1 + \frac{1}{g} \exp \frac{(E_D - E_F)}{KT}} \right] \qquad (8)$$

Similarly when acceptor impurities of concentration $N_A(cm^{-3})$ are added

$$N_A^- = \frac{N_A}{1 + g \exp \frac{(E_A - E_F)}{KT}} \qquad (9)$$

where

g = ground state degeneracy of donor/acceptor

g = 2 for donor impurity in (G_e and S_i)

= 4 for accepter impurity in (Y_e and S_i)

when impurity atoms are added, the n.p. product is still given by eqn. (6). At relatively elevated temperature most donor and acceptors are ionised.

$$n + N_A = p + N_D \qquad (10)$$

From equation (6) and (10) concentration of electrons and holes in a n type semiconductor

$$n_{no.} = \frac{1}{2}\left[(N_D - N_A) + \sqrt{(N_D - N_A)^2 + 4 n_i^2}\right] \qquad (11)$$

$$p_{no.} = \frac{n_i^2}{n_{no}} \quad \frac{n_i^2}{N_D}$$

$$\text{and } E_C - E_F = KT \ln \left(\frac{N_C}{N_D}\right) \qquad (12)$$

$$E_F - E_i = KT \ln \left(\frac{n_{no}}{n_i}\right) \qquad (13)$$

Similarly the concentration of holes and electrons in a p type semiconductor is given by

$$p_{po} = \frac{1}{2}\left[(N_A - N_D) + \sqrt{(N_A - N_D + 4n_i^2)}\right] \qquad (14)$$

$$n_{po} = \frac{n_i^2}{p_{po}} \quad \frac{n_i^2}{N_A} \qquad (15)$$

$$E_F - E_V = KT \ln \left(\frac{N_V}{N_A}\right) \qquad (16)$$

$$E_i - E_F = KT \ln \left(\frac{p_{po}}{n_i}\right) \qquad (17)$$

Consider a metal insulator semiconductor structure of Fig. 17. The thickness of the insulator is d and v is the applied voltage on the metal plate.

P TYPE

N-TYPE

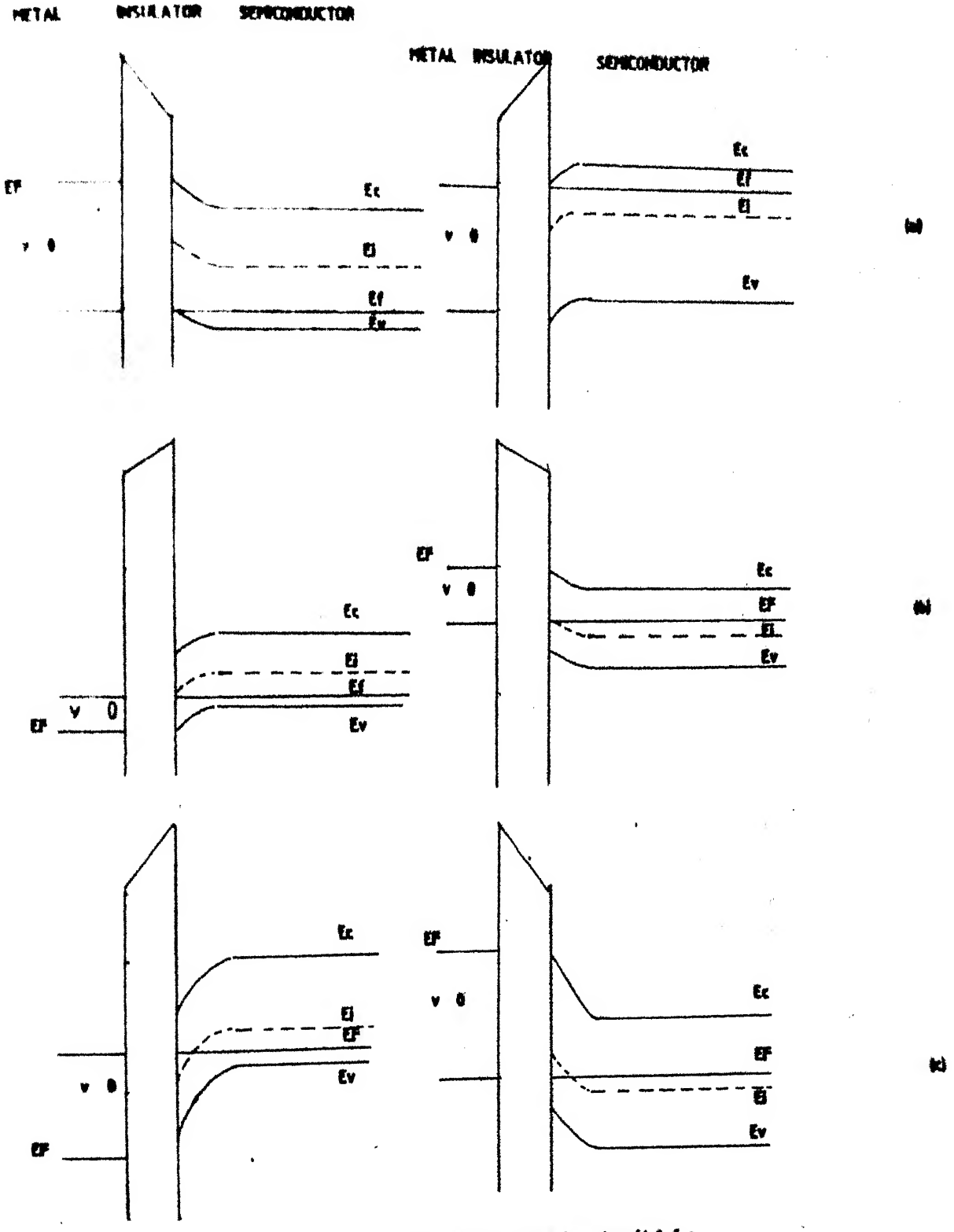

Energy - band diagrams for ideal MIS diodes when V=0 for

a) Accumulation
b) Depletion
c) Inversion

Let

ψ_s = surface potential at the semiconductor surface w.r.t. E_i

ψ_B = potential difference between the Fermilevel E_F and intrinsic Fermilevel E_i

when the MIS structure of Fig.17 is biased with positive or negative voltage, basically three cases may exist

i) Accumulation

ii) Depletion

iii) Inversion

The effect of applied bias and consequent band bending is illustrated in Fig. 4. Briefly we have the following cases for a p type semiconductor

$\psi_s < 0$ accumulation of holes

$\psi_s = 0$ flat band condition

$\psi_B > \psi_s > 0$ depletion of holes (band bend downward)

$\psi_s = \psi_B$ mid gap with $n_s = p_s = n_i$ (intransic concentration)

At the surface the electron and hole density are given by

$$n_s = n_{po} \exp(\beta \psi_s) \tag{18}$$

$$p_s = p_{po} \exp(-\beta \psi_s) \tag{19}$$

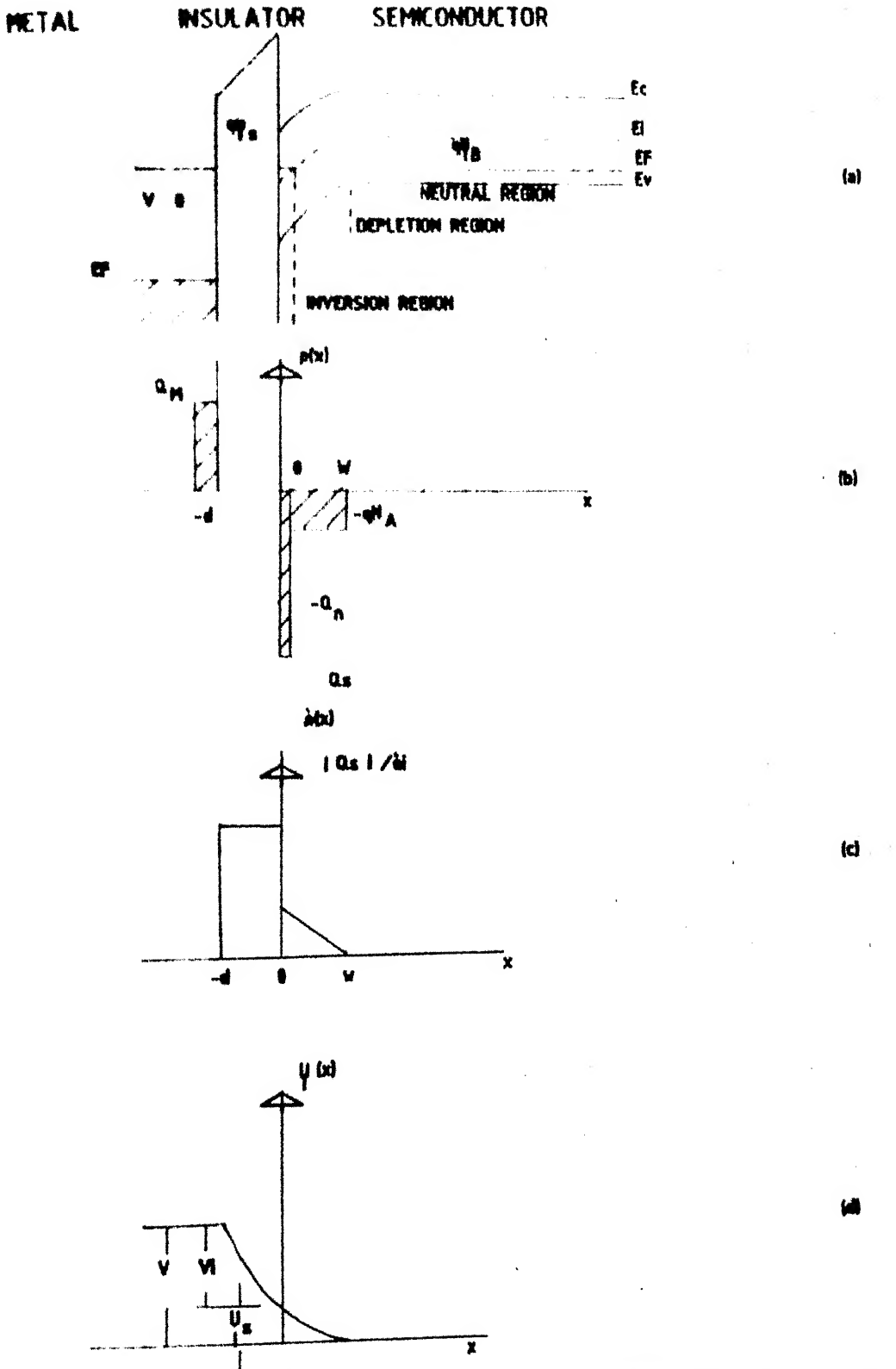

(a) Band diagram of an ideal MIS diode
(b)Charge distribution in inversion
(c) Electric field distribution
(dPotential distribution

FIG- 18

where

$$B = \frac{KT}{q}$$

n_{po} = equilibrium electron density

p_{po} = equilibrium hole density

ψ_s is essentially the measure of bend in E_i at the surface of the semiconductor

Fig.17 shows the band diagram of a MIS structure with the band bending of the semiconductor (p type). The charge distribution is shown in Fig. 18(b). For charge neutrality of the system it is required that

$$Q_M = Q_n + q N_a W = Q_s \qquad (20)$$

where Q_M = charge/unit area on the metal

Q_n = electron/unit area in the inversion layer

$q N_a W$ = ionised acceptor/unit area in the space charge space charge width W and

Q_s = total charge/unit area in the semiconductor

In absence of any work function difference the applied voltage partly appear across the insulater and partly across the silicon. Thus

$$V = V_i + \psi_s \qquad (21)$$

and $$V_i = \mathcal{E}_i d = \left| \frac{Q_s | d}{\mathcal{E}_i} = \left| \frac{Q_s}{C_i} \right| \right. \qquad (22)$$

Another quantity of interest is the turn on voltage V_T at which the strong inversion occurs and is given by

$$V_T(\text{strong inversion}) = \frac{Q_s}{C_i} + 2\psi_B \qquad (23)$$

Also for strong inversion

$$\psi_s = 2\psi_\beta \qquad (24)$$

Also at the on set of strong inversion

$$Q_s = q N_a W \text{ from eqn. (20)}$$

The turn voltage therefore

$$V_T = \sqrt{\frac{2\varepsilon_s q N_A 2\psi_\beta}{C_i}} + 2\psi_\beta \qquad (25)$$

also since the surface potential

$$\psi_s = \frac{q N_a W^2}{2\varepsilon_s} \qquad (26)$$

the space charge width

$$W = \frac{\sqrt{2\varepsilon_s \psi_s}}{q N_a} \qquad (27)$$

The above discussion helps provide the physics of MOS device and provides the basis for formulation of any model.

APPENDIX B

THE LEVENBERG-MARQUARDT ALGORITHM

The algorithm essentially is the implementation of matrix equation

$$(J^T J + \lambda D^2)\Delta A = J^T [Y-Y^*]$$

STEP — DESCRIPTION

0 Enter b[i]; i=1,2,...n, the starting values of the parameters.

Enter NN, the no. of data points.

Enter minm, a small no. such as the machine precision to which the Marquardt parameter, lambda, is to be set, should it have underflowed.

Let inc = 10 be the factor to increase lambda

Let dec = 0.4 be the factor to decrease it

Let lambda = .001 be the initial value of Marquardt parameter.

Let phi = 1 be the value of quantity used by NASH to avoid singularity.

Enter EPS = The convergence criteria for least square objective function.

Enter GAMA = The convergence criteria for change in parameters between successive iterations.

STEP	DESCRIPTION
	Enter function
	Enter analytical derivatives
1	Compute S the current objective function
2	Compute J^T, $J^T J$,
3	Compute [Y-Y*] thru 'function'
4	Compute J^T [Y-Y*].
5	Compute $(J^T J + D^2)$
6	Solve for A
7	Compute $\underline{A}$ new = $\underline{A}$ old + $\underline{A}$
8	Compute R the new objective function
9	If convergence criteria satisfied 'stop' [12].
10	If (R.LT.S) = dec and Go to 1.
11	If (R.GT.S) = inc and Go to 1.
12	STOP
13	END

Appx C

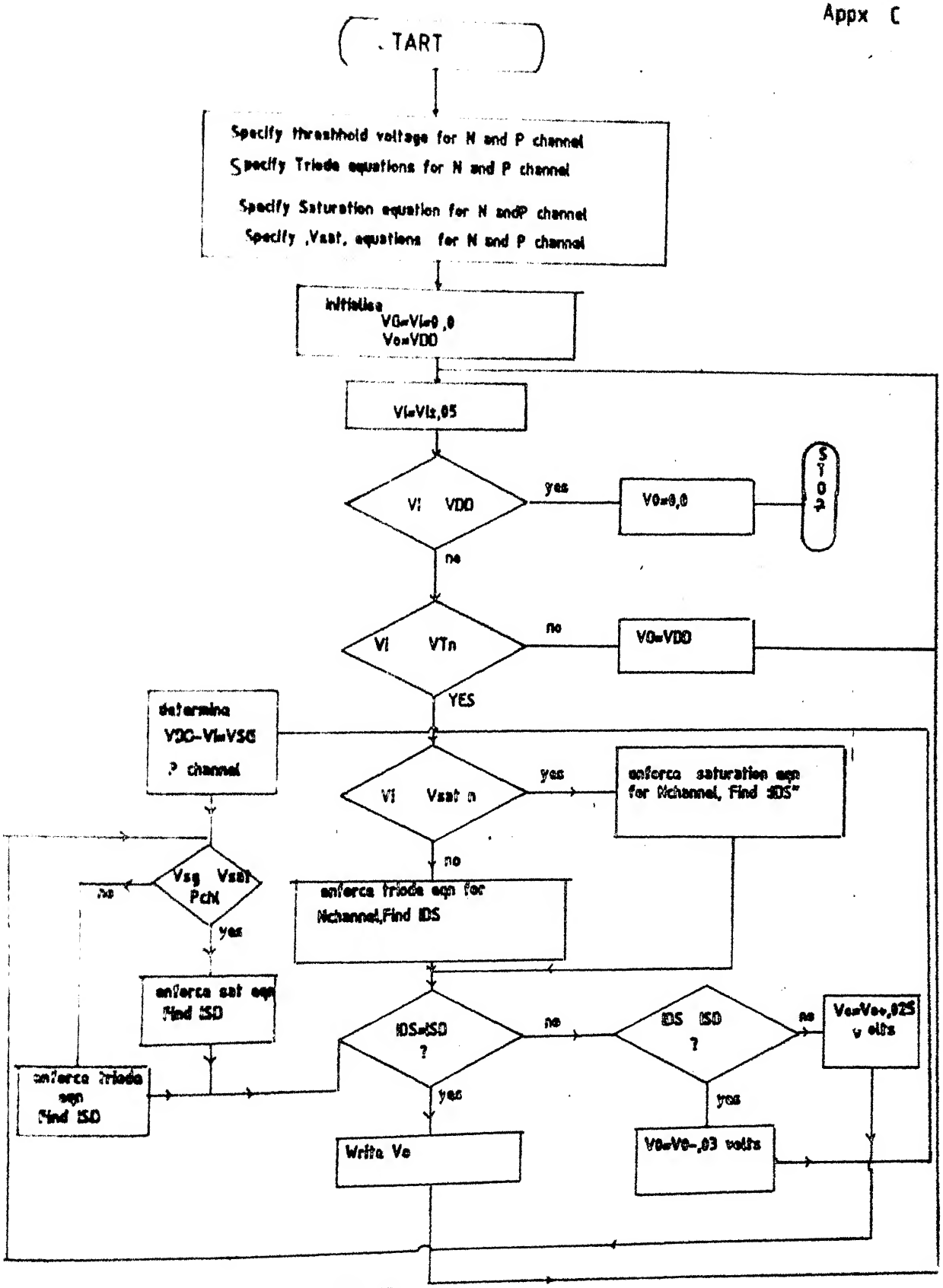
TART
Specify threshhold voltage for N and P channel
Specify Triode equations for N and P channel
Specify Saturation equation for N andP channel
Specify ,Vsat, equations for N and P channel
initialise
VG=Vi=0 ,0
Vo=VDD
Vi=Vi+,05
Vi VDD
yes
V0=0,0
STOP
no
Vi VTn
no
V0=VDD
YES
determine
VDD-Vi=VSG
P channel
Vi Vsat n
yes
enforce saturation eqn
for Nchannel, Find IDS"
no
enforce triode eqn for
Nchannel,Find IDS
Vsg Vsat
Pch
no
yes
enforce sat eqn
Find ISD
IDS=ISD
?
no
IDS ISD
?
no
Vo=Vo+,025
v olts
enforce triode
eqn
Find ISD
yes
yes
Write Vo
V0=V0-,03 volts

FIG-19

THE CMOS CONFIGURATION (CD-4007)

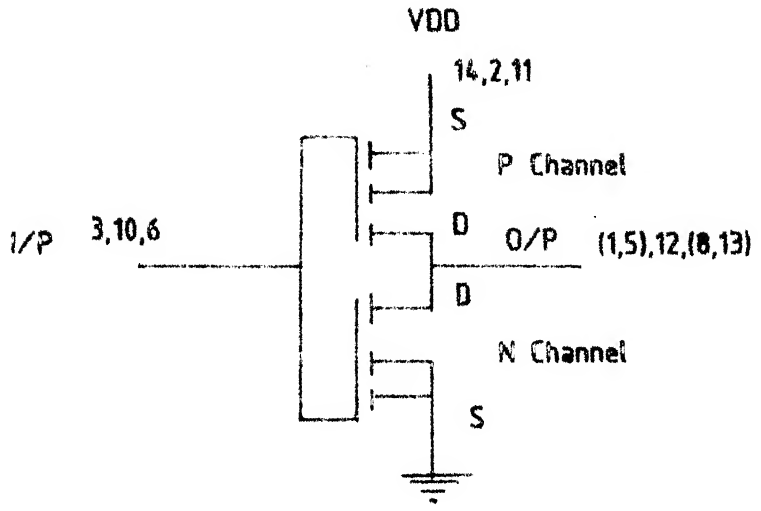

FIG -19 b

PIN CONFIGURATION (CD-4007)

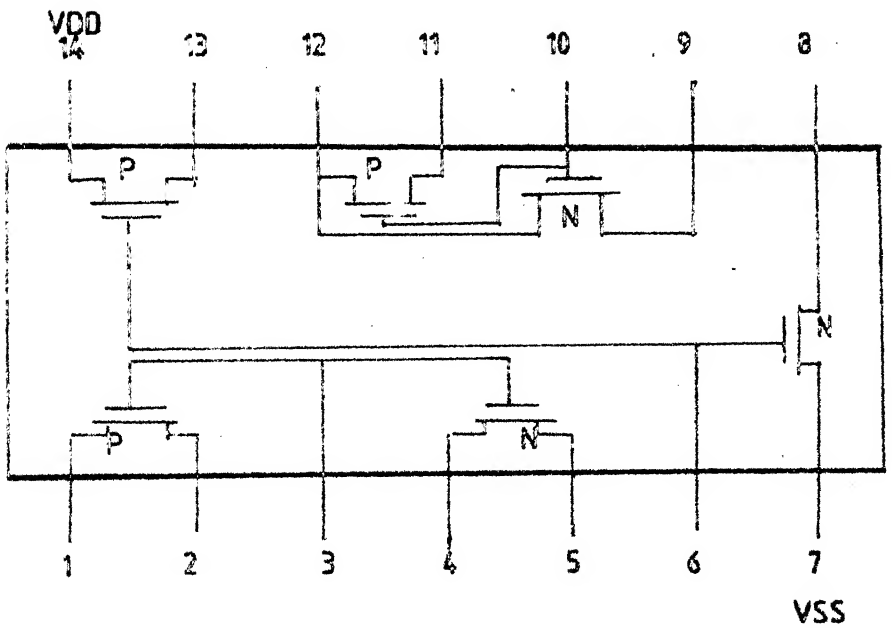

FIG-20

APPENDIX D

SPECIFICATIONS OF DEVICE UNDER STUDY

The device under study is CD4007 (Dual complementary pair plus a CMOS inverter). The pin diagram of the chip is as given in Fig. 20.

The chip comprises of three complementary pairs of N channel and P channel enhancement mode MOSFETS. All inputs are protected by diode clamps For proper operation voltages at all pin must be constrained to (VSS-.3V) and (VDS + .3V). The supply voltage range can vary from 3.0V-15V.

The physical parameter of the device are listed below.

N Channel

$W = 7.5$ mil $\qquad V_{tx} = 0.8$

$L = 0.15$ mil $\qquad 2Qf_{N\ chl} = \frac{kT}{q} \ln \frac{NA}{n_i} = 0.74$/at $300^{\circ}K$

$T_{ox} = 1200A^{\circ}$ $\qquad K = \frac{\mu E_{ox} W}{2LT_{ox}} = .309E\text{-}3\ A/V^2$

$\mu = 420\ cm^2/V\ sec$ $\qquad R = \frac{T_{ox}}{E_{ox}} \sqrt{2qE\ S_i N} = 3.306V^{1/2}$

$N = 2.8 \times 10^{16} cm^{-3}$

$E_{ox} = 4$

$E_{si} = 12$

For P Channel

$W = 19.5$ mil

$L = 0.25$ mil

$T_{ox} = 1200^{\circ}A$

$\mu = 165\ cm^2/V\ sec$

$N = 3 \times 10^{15}\ cm^{-3}$

$V_{tx} = 0.68$

$2\phi f_{P\ chl} = \frac{kT}{q}\left(n\frac{N_D}{n_i}\right) = 0.62$ at $T=300^{\circ}K$

$K = \frac{\mu E_{ox} W}{2LT_{ox}} = .189E\text{-}3\ \mu A/V^2$

$K_p = \frac{T_{ox}}{E_{ox}} \sqrt{2q\ E_{si} N} = 1.082\ V^{1/2}$

REFERENCES

1. MOS Models and Circuit Simulation
   - John E. Meyer. RCA Review, vol. 32, Mar 71 pp. 42-63.

2. Optimisation techniques with FORTRAN
   - James L. Kuester, Joe H. Mize, McGraw Hill.

3. Compact Numerical Methods for Computers
   - J.C. Nash, Adam Hilger Ltd., Bristol.

4. Modified 1/f Trapping Noise Theory and Experiment in MOS transistors biased from Weak to Strong Inversion
   - G. Reimbold, IEEE Trans. on Electron Devices, vol. ED-31, No. 9, Sept. 1984.

5. Optimised Extraction of MOS Model Parameters,
   - D.E. Ward and K. Doganis, IEEE Trans. on CAD, CAD-1, No. 4, Oct. 1982, p. 163.

6. General Optimisation and Extraction of IC Devices Model Parameters
   - K. Doganis and D.L. Scharfetter, IEEE Trans. on Electron Devices, ED-vol. 30, Sept. 1983.

7. Electron Mobility in Inversion and Accumulation Layers, on Thermally Oxidised Silicon Surfaces
   - S.C. Sun and James D. Plummer, IEEE Trans. on Electron Devices, vol. ED-27, No. 8, Aug. 1980.

EE-1985-M-DAS-COM